



# The Geoengineering Model Intercomparison Project (GeoMIP) contribution to CMIP7 - description of new experimental protocols and preliminary results

Daniele Visoni<sup>1</sup>, Alan Robock<sup>2</sup>, Alistair Duffey<sup>3</sup>, Matthew Henry<sup>4</sup>, Haruki Hirasawa<sup>5</sup>, Walker Raymond Lee<sup>6</sup>, Cindy Wang<sup>1</sup>, Kelsey Roberts<sup>1</sup>, Shingo Watanabe<sup>7,8</sup>, Michelle Simões Reboita<sup>9</sup>, Masahiro Sugiyama<sup>10</sup>, Ben Kravitz<sup>11</sup>, Jim Haywood<sup>4</sup>, Simone Tilmes<sup>12</sup>, Frédéric K. Bonou<sup>13</sup>, Jack Chen<sup>6</sup>, Timofei Sukhodolov<sup>14</sup>, Sandro Vattioni<sup>14,15</sup>, Andrin Jörimann<sup>14,15</sup>, Diego Villanueva<sup>15</sup>, Ryan Vella<sup>15</sup>, Paul Farron<sup>15</sup>, Ewa Bednarz<sup>16,17</sup>, Ulrike Niemeier<sup>18</sup>, Colleen Golja<sup>19</sup>, and Juan A. Añel<sup>20</sup>

<sup>1</sup>Department of Earth and Atmospheric Sciences, Cornell University, Ithaca, NY, 14850 USA

<sup>2</sup>Department of Environmental Sciences, Rutgers University, New Brunswick, NJ, USA

<sup>3</sup>Reflective, San Francisco, CA, United States

<sup>4</sup>Department of Mathematics and Statistics, University of Exeter, Exeter, UK

<sup>5</sup>Department of Atmospheric and Climate Sciences, University of Washington, Seattle, WA, 98105 USA

<sup>6</sup>Climate & Global Dynamics Laboratory, NSF National Center for Atmospheric Research, Boulder, CO, 80305

<sup>7</sup>Japan Agency for Marine-Earth Science and Technology (JAMSTEC), Yokohama, Kanagawa, Japan

<sup>8</sup>Advanced Institute for Marine Ecosystem Change (WPI-AIMEC), Tohoku University, Sendai, Japan

<sup>9</sup>Instituto de Recursos Naturais, Universidade Federal de Itajubá, Itajubá, Brazil

<sup>10</sup>University of Tokyo, Tokyo, Japan

<sup>11</sup>Department of Earth and Atmospheric Sciences, Indiana University, Bloomington, IN, USA

<sup>12</sup>National Science Foundation - National Center for Atmospheric Research (NSF-NCAR), Atmospheric Chemistry Observations & Modeling (ACOM), Boulder, CO, USA

<sup>13</sup>Institut de Recherches Halieutiques et Océanologiques du Bénin (IRHOB), Benin

<sup>14</sup>Physikalisch Meteorologisches Observatorium Davos/World Radiation Center, Davos, Switzerland

<sup>15</sup>Institute for Atmospheric and Climate Science, ETH Zurich, Zurich, Switzerland

<sup>16</sup>Cooperative Institute for Research in Environmental Sciences (CIRES), University of Colorado at Boulder, Boulder, CO, USA

<sup>17</sup>NOAA Chemical Sciences Laboratory (NOAA CSL), Boulder, CO, USA

<sup>18</sup>Max Planck Institute for Meteorology, Hamburg, Germany

<sup>19</sup>Department of Physics, Imperial College London, London, UK

<sup>20</sup>EPhysLab, CIM-UVigo, Universidade de Vigo, Ourense, Spain

**Correspondence:** Daniele Visoni (dv224@cornell.edu)

**Abstract.** The Geoengineering Model Intercomparison Project (GeoMIP) is a coordinated international model intercomparison effort with the aim of providing robust experimental protocols for simulations of various Solar Radiation Modification (SRM) methods. Through many iterations and discussions within the GeoMIP community, it has become clear that balancing simplicity with scientific realism and policy relevance and associated complexities is fundamental when designing modeling experiments.

- 5 Such experiments must both diagnose areas of model agreement and disagreement through the lens of climate science and provide results useful for understanding the potential downstream impacts of SRM across different sectors. Here we present a suite of new climate model experiments designed for the Coupled Model Intercomparison Project Phase 7 (CMIP7), building



on lessons learned from previous GeoMIP experiments, recent SRM research, and new simulations developed for CMIP7. We provide detailed experimental designs and their underlying rationale, including preliminary results from sensitivity analyses performed with CMIP6 models. Compared to previous GeoMIP iterations, we organize experiments into three categories: 10 i) Preparatory Experiments, designed to diagnose model responses and inform more complex experimental designs; ii) Tier 1 experiments, the core simulations that all participating models are encouraged to run; and iii) Tier 2 experiments, which provide a flexible framework for exploring structural and scenario uncertainties under SRM, including the potential interaction with temporary overshoot scenarios and tipping elements dynamics. This framework encourages modeling groups to propose 15 their own experiments building upon the Tier 1 backbone, enabling more targeted exploration while ensuring cross-model compatibility.

## 1 Introduction

Solar Radiation Modification (SRM, also known as solar geoengineering or climate intervention) encompasses a broad category of theoretical methods that aim to affect Earth's energy balance with the goal of potentially reducing the impacts of anthropogenic global warming. Many of these methods are based on real-world analogues that suggest such interventions 20 could be effective, either regionally or globally.

Stratospheric Aerosol Injection (SAI) is inspired by observations of large explosive volcanic eruptions, such as Mt. Pinatubo in 1991, in which sulfate aerosols or their precursors are injected in the stratosphere, reflecting a portion of incoming sunlight before it reaches the troposphere and thereby cooling the planet. Marine Cloud Brightening (MCB) is inspired by observations 25 of increased cloud albedo due to aerosol shipping emissions and lower-atmospheric injections of sulfate from some volcanic eruptions, leading to an increase of Earth's albedo through cloud brightness and other cloud changes. Proposals for Cirrus Cloud Thinning (CCT) or Mixed-phase Cloud Thinning (MCT) arise from observations of the warming impact of tropospheric ice clouds, and questions if their coverage could be reduced in order to allow for more terrestrial radiation to escape to space.

The known natural events that inspire these proposals suggest they could be replicated artificially, though with obvious engineering challenges (Smith, 2024). However, a broad understanding of the basic physical principles behind such analogues 30 does not necessarily provide a deeper understanding of how effective these methods could be in the real world—both in terms of their actual capacity to reduce surface temperatures and in terms of the downstream ramifications of a given cooling source. Both issues can be investigated through the use of climate models of different complexities, from simpler Energy Balance Models (EBMs) to highly complex Earth System Models (ESMs). Over the last 25 years of research within this field, such 35 climate models have shown that none of those methods can simply “turn back the clock” (Vioni et al., 2021b), reverting the climate to the same state that it was in before temperatures rose due to rising greenhouse gases. Models differ across various components of the projected response to SRM (Haywood et al., 2025) and in their assessment of the methods' efficacy, due to a combination of model structural differences, parametric uncertainty, and different assumptions in how perturbations are represented as well as lack of inclusion of certain key underlying physical, chemical or natural processes in the models 40 (Eastham et al., 2025). Nevertheless, they have also shown that in scenarios in which further warming is prevented through



SRM in more or less idealized ways, and in which the cooling is maintained over time and is somewhat uniform in nature, key climatic risks could be reduced (Irvine et al., 2019; Tye et al., 2022; Wells and Haywood, 2025), albeit not always uniformly geographically (Feng et al., 2025; Egbebiyi et al., 2025). Additionally, research has identified non-negligible secondary impacts or “unintended consequences” arising from the application of such methods, for instance on atmospheric composition (Tilmes et al., 2022; Bednarz et al., 2025b). It is important to acknowledge the limitations of preliminary assessments on various fronts. Firstly, on the scenario front, the assessment of uniform, constant deployment may neglect considerations of irregularities in the potential deployment over time (Trisos et al., 2018) or over potential asymmetries (Haywood et al., 2023). Secondly, on the modeling front, many of these assessments may over-rely on one or few models, under-representing uncertainties (Henry et al., 2023), or the models may lack the spatial resolution necessary to correctly capture regional dynamics (Sun et al., 2025), or key processes altogether, for instance in the ecological sphere (Zarnetske et al., 2021). These known limitations reinforce the importance of a systematic approach to coordinating modeling efforts.

The Geoengineering Model Intercomparison Project (GeoMIP) is a coordinated, international effort with the aim of providing robust experimental protocols for Earth system model (ESM) simulations of various SRM methods. This coordination has three main identifiable goals: 1) enabling a better understanding of inter-model differences in SRM simulations, by ensuring experimental protocols are as detailed and well documented as possible to reduce potential divergence arising from differences in the modeling set-up; 2) offering a standardized framework of simulations for the purpose of broader assessments of SRM, making sure decisions around experimental details are taken by a broad, representative community that includes modelers, climate researchers, researchers interested in potential downstream impacts of SRM (including on agriculture, society, infrastructure and ecological systems) that is capable of weighing and documenting different needs and opinions; 3) supporting the community of users by facilitating data sharing practices and coordinating analyses. GeoMIP facilitates this coordination both by organizing annual workshops, where researchers can both present their recent findings and discuss future steps, and for which reports are publicly made available every year (see, for instance, Vioni et al. (2025) for the meeting held in 2025 where many of the decisions reported in this document were taken), as well as coordinating with the broader Climate Model Intercomparison Project (CMIP) and World Climate Research Program (WCRP) community to ensure relevance and compliance with best practices, for instance informing efforts to better coordinate data requests for the most important variables for analyses (Juckes et al., 2025).

A review of GeoMIP’s role and efforts over the years, including a detailed list of experiments performed by the community, as well as lessons learned by previous experiments, was provided in Vioni et al. (2023c). Since then, the community has continued discussions around future experiments to run as part of the phase 7 of CMIP (CMIP7), considering both recent advances in understanding the design space of different SRM techniques and models’ development (such as the potential inclusion of an interactive carbon cycle in CMIP7 models) as well as changes in other MIPs of relevance (for instance, the Scenario Model Intercomparison Project, ScenarioMIP). In particular, in Vioni et al. (2024) a new, intermediate experimental protocol was proposed, noting that the original CMIP6 protocol described in Kravitz et al. (2015) required some updates that would have



enabled continued policy relevance and connection to other MIPs on the scenario side as well as updating the potential intervention strategies to be simulated based on the most recent research. As an example, the original G6sulfur experiment simulated initialization of SRM in 2020 and simulated the intervention under the Shared Socioeconomic Pathway (SSP) scenario 5-8.5, whose relevance and plausibility has been hotly contested (Burgess et al., 2020; Schwalm et al., 2020).

80

In this paper, we describe the set of experiments decided by the GeoMIP community for CMIP7, detailing both the underlying reasoning behind the specific decisions as well as providing as much guidance as possible for modeling teams. We describe first what we call the "Preparatory experiments" in Section 2, which are shorter, more technical idealized simulations to enable the design of the main CMIP7 simulations, traditionally termed "Tier 1", which are described in Section 3; followed by a description of a broader range of experiments termed "Tier 2" that both aim to expand the range of potential scenarios under analyses as well allowing for some more tentative experiments, in Section 4.4.

85

## 2 Preparatory experiments

Before running the main Tier 1 experiments, modeling teams are advised to run these simpler, shorter experiments that allow for a better diagnosis of the models' responses to the Tier 1 experiments, as well as clarifying the models' sensitivities to the interventions. Consistently defined preparatory experiments serve to both enable clearer assessment of process differences across models and provide a template to simplify the preparation for the Tier 1 simulations based on past modeling experience. A detailed explanation of all these experiments, listed in Table 1, is provided in the following subsections.

90

### 95 2.1 Single point injection location SAI simulations

Modeling centers aiming to run the G7-1.5K-SAI (and similar) simulations should consider performing single point injection (SPI) simulations of 12 Tg-SO<sub>2</sub> for a number of years (10 year is the minimum, 35 years is suggested) at specific latitudes, using the same fully-coupled atmosphere-ocean configuration as the one they plan to use for G7-1.5K-SAI. SPIs at 30°N, 15°N, 15°S, 30°S were already proposed as a testbed experiment in CMIP6 in Visioni et al. (2023a) in order to understand models' sensitivities to different injection locations and to allow for the calculations necessary to devise the feedback controller (MacMartin et al., 2017). These simulations have been shown to be very informative in diagnosing models' response to SAI, for instance helping understand how the evolution of the aerosol plume affect the Atlantic Meridional Overturning Circulation (AMOC) or Arctic sea ice (Bednarz et al., 2025a; Kim et al., 2025), as well as to train climate emulators capable of better spanning the space of SAI strategies (Farley et al., 2026). For CMIP7, the set has been expanded to include injections at 60°N and 60°S for the High Latitude, Low Altitude (HiLLA) simulations, and given earlier results from Lee et al. (2023) and Duffey et al. (2025) at an altitude of 15 km, whereas injections at 30°N and 30°S should be performed at an altitude of 21.5 km as described in Richter et al. (2022). The injection longitude is not as important for injections significantly above the tropopause

100

105



Experiment name	Description of intervention	Underlying emission scenario	Period
Preparation for G7-1.5K-HiLLA experiment			
Inj-sulf-60N	SPI of 12 Tg-SO <sub>2</sub> at 60°N during MAMJ, at 15 km height	ML	2035, min 10 years
Inj-sulf-60S	SPI of 12 Tg-SO <sub>2</sub> at 60°S during SOND, at 15 km height	ML	2035, min 10 years
Preparation for G7-1.5K-SAI experiment			
Inj-sulf-30N	SPI of 12 Tg-SO <sub>2</sub> at 30°N yearly, at 21.5 km height	ML	2035, min 10 years
Inj-sulf-30S	SPI of 12 Tg-SO <sub>2</sub> at 30°S yearly, at 21.5 km height	ML	2035, min 10 years
Preparation for other SAI experiments and training emulators			
Inj-sulf-15N	SPI of 12 Tg-SO <sub>2</sub> at 15°N yearly, at 21.5 km height	ML	2035, min 10 years
Insta-sulf-15N	Instantaneous injection of 12 Tg-SO <sub>2</sub> using the same details as Inj-sulf-15N	ML	2035, min 5 years
Inj-sulf-15S	SPI of 12 Tg-SO <sub>2</sub> at 15°S yearly, at 21.5 km height	ML	2035, min 10 years
Inj-sulf-XN/S	SPI of 12 Tg-SO <sub>2</sub> at another latitude yearly, at 21.5 km height	ML	2035, min 10 years
	if needed to expand exploration of SAI strategies	ML	2035, min 10 years
Preparation for G7-1.5K-MCB experiment			
Inj-seasalt-midlat-SST	SSI in 5 midlat regions of 100 Tg yr <sup>-1</sup> split equally in mass between hemispheres	fixed SST	min 5 years
Inj-seasalt-midlat	SSI in 5 midlat regions of -2 W/m <sup>2</sup> split equally in mass between hemispheres	ML	min 20 years
Total: At least 8 experiments			At least 105 years

**Table 1.** Process understanding, preparatory experiments to help run and interpret the Tier 1 experiments. SPI = Single Point Injections; MAMJ = March, April, May, June; SOND = September, October, November, December; SSI = Sea salt injections, values refer to the injection rate of NaCl which is typically around 3.5 % in sea-water; SST = sea surface temperature; ML = Medium-Low scenario. The last row shows the total number of experiments and the minimum number of years of simulation (one ensemble member is sufficient).

(Sun et al., 2023), but for consistency injections should be all at 0°E.

110 To be most useful, modeling teams running this set of preparatory experiments should also include diagnostics that help evaluate how injection location shapes regional climate systems. This could include metrics that enable the evaluation of changes in monsoon rainfall, Arctic sea ice, and the AMOC, as well as hydrological cycle changes in subtropical and equatorial regions. Such diagnostics can help identify model dependent sensitivities and clarify the extent to which injection strategies can minimize disruptions while achieving the desired cooling target. Preparatory experiments also provide an opportunity to test

115 the robustness of SRM strategies across diverse climate models. By systematically analysing responses across regions, they ensure that future SRM assessments can incorporate perspectives from different climates and socio-economic contexts, rather than focusing only on global averages. This broader approach strengthens the scientific foundation of Tier 1 experiments and



enhances their relevance for both science and policy.

120 Modeling centers should also consider running a version of the 15°N case (Inj-sulf-15N) with the same yearly amount (12 Tg-SO<sub>2</sub>), location and height (22.5 km), but where the injection is instantaneous, on January 1st, in order to also provide a comparison of pulse versus continued injection impacts (Plazzotta et al., 2018), and that could provide a point of comparison with volcanic-related MIPs such as VolMIP (Zanchettin et al., 2022) and ISAMIP (Quaglia et al., 2023).

125 Models can also perform simulations at other latitudes than the ones listed, as done for instance in Zhang et al. (2022), to understand the potential limits of the design space. SPI simulations have shown great promise as training elements for SAI climate emulators (Farley et al., 2026), and extending the range of SPI simulations could provide further training data to improve and expand the exploration of different scenarios beyond what is feasible to do with ESMs.

## 130 2.2 Midlatitude MCB benchmarking simulations

MCB simulations for GeoMIP7 focus on a strategy in which MCB accumulation-mode sea salt aerosol emissions are emitted at the ocean surface in five mid-latitude ocean regions, with emission rates set to produce equal areal-sum emissions in each hemisphere, following recent testbed simulations (Hirasawa et al., 2026, 2025a) (see discussion and region definitions in section 3.4). To prepare for the G7-1.5K-MCB scenario simulations, modelers should conduct two benchmarking simulations aimed  
135 at characterizing the cloud susceptibility and climate response to mid-latitude MCB: Inj-seasalt-midlat-SST and Inj-seasalt-midlat. This two-stage approach is motivated by model intercomparison work showing large differences in the aerosol-cloud forcing susceptibility to MCB sea salt aerosol emissions (Stjern et al., 2018; Rasch et al., 2024) due to differences in the size distribution of aerosol emissions and aerosol-cloud process uncertainty. Thus, in contrast to the SAI preparatory simulations, we request that modelers first estimate the effective radiative forcing from MCB using a fixed sea surface temperatures simulation  
140 (Inj-seasalt-midlat-SST). This simulation should use present-day SST and emission fields if possible and we recommend an initial emission rate of 100 Tg yr<sup>-1</sup> of NaCl, which falls roughly within the emission rates found in Alterskjaer et al. (2013) and Hirasawa et al. (2026). In addition to easing the benchmarking process, consistently defined fixed SST simulations will be necessary for conducting process analysis studies to understand aerosol, cloud, and other processes that cause inter-model differences in MCB efficacy that are crucial for improving process understanding, identifying model deficiencies, and con-  
145 straining the potential forcing from MCB.

The magnitude of MCB forcing is strongly dependent on the details of the sea salt aerosols, particularly the size distribution of the emitted aerosol as the aerosol indirect effect depends on the aerosol number flux rather than the mass flux (Rasch et al., 2024). Previous ESM and parcel modeling work has identified accumulation mode aerosol as the most effective size to achieve  
150 cloud brightening (Alterskjær and Kristjánsson, 2013; Wood, 2021) with approximate effective dry radii of 30 nm to 50 nm, depending on the activation parameterization. We recommend modelers use sea salt emissions in this size range, though we



recognize this may not be strictly possible depending on sea salt emission parameterization implementation. MCB scenario simulations have been successfully completed with sea salt aerosol effective radii of up to 180 nm. However, emission size can drive large variations in the sea salt aerosol mass required across the models (Hirasawa et al. (2025a), Fig. 5a), meaning careful documentation of the emitted sea salt size distribution is necessary to compare models' responses, as the inter-model range tends to decrease when considering the number flux instead (Fig. 3b).

Using the information from this simulation, modelers should then conduct a coupled simulation to estimate the climate response sensitivity to MCB (Inj-seasalt-midlat). This simulation is patterned on previous GeoMIP MCB simulations, G4cdnc and G4sea-salt (Kravitz et al., 2013; Ahlm et al., 2017), with a Medium-Low (ML) emission scenario as a reference case and a time-constant MCB emission rate applied from 2035 to 2075. In contrast to previous simulations, we prescribe a target forcing ( $-2 \text{ W m}^{-2}$ ), rather than a predetermined emission rate or droplet number enhancement. The MCB aerosol-cloud forcing is non-linear, however a linear assumption is likely sufficient to provide a reasonable estimate of the climate sensitivity. Thus, we recommend setting the emission rate to  $100 \text{ Tg yr}^{-1} \times (-2 \text{ W m}^{-2} / \text{ERF}_{100\text{Tg}})$ , where  $\text{ERF}_{100\text{Tg}}$  is the effective radiative forcing computed from Inj-seasalt-midlat-SST. The temperature response derived from this simulation will then enable modelers to design and conduct the G7-1.5K-MCB simulations.

### 3 Tier 1 CMIP7 experiments

The Tier 1 experiments are higher-priority fully coupled experiments that all modeling teams are encouraged to run. The underlying framework behind the scenario choices has been explained in detail in Visoni et al. (2024) for the experiment G6-1.5K-SAI. Visoni et al. (2024) was meant to both collect the thoughts and opinions of the GeoMIP community about what constitutes a broadly agreed upon, policy-relevant SRM experiment and to devise an experiment that could be run with some consistency with CMIP6 models and with CMIP7 models, in order to compare more easily across models' generations. This meant avoiding too high GHG emission scenarios that might not have a CMIP7 counterpart, as well as being considered less realistic, and selecting a scenario that was more consistent with current and near-term future emission trajectories: for CMIP6, that entailed selecting SSP2-4.5 (Burgess et al., 2020), whereas during the Fifteenth GeoMIP workshop (Visoni et al., 2025) the ML scenario was selected as the CMIP7 counterpart.

This also meant anchoring the SRM target to a clearly defined metric that could be consistent between simulations with concentration-driven  $\text{CO}_2$  and simulations with emission-driven  $\text{CO}_2$ . For this reason, the goal of the Tier 1 CMIP7 simulations, just like the CMIP6 ones, is to deploy SRM to maintain global mean temperatures at  $1.5^\circ\text{C}$  above Preindustrial. The definition of  $1.5^\circ\text{C}$  above Preindustrial (PI) is somewhat different from what is usually used: after testing and analyses, it was decided to anchor the definition of  $1.5^\circ\text{C}$  above PI for the purpose of the simulations' target to each model's average global mean surface air temperatures (GMSAT) in the period 2020-2039. This rationale has been explored in Visoni et al. (2024); mainly, models' actual PI temperatures diverge greatly, and so does the period 1850-1900, which is usually used as a reference timeframe in the IPCC and other assessments. On the other hand, anchoring the target to the actual models' near-present time temperatures



Experiment name	Description of intervention	Underlying emission scenario	Period
G7-1.5K-SAI	Equal daily injections of SO <sub>2</sub> at 30°N and 30°S for the whole year to maintain GMSAT at 1.5°C above PI	ML	2035-2150
G7-1.5K-SAI-End	Termination of G7-1.5K-SAI in 2085	ML	2085-2100
G7-1.5K-HiLLA	Equal daily injections of SO <sub>2</sub> , 60°N (during MAMJ) and 60°S (during SOND) to maintain GMSAT at 1.5°C above PI	ML	2035-2150
G7-1.5K-MCB	Injections of sea salt aerosols in five midlatitude regions with equal mass in both hemispheres to maintain GMSAT at 1.5°C above PI	ML	2035-2150
Total: 3 experiments			345 years PEM

**Table 2.** Tier 1 experiments for GeoMIP7. Specific details about the experimental set-ups and their justifications are provided in the text; Determination of injection amounts in the experiments to be performed through a 1 Degrees-of-freedom (DOF) feedback controller as discussed in (Kravitz et al., 2016; Lee et al., 2025a). GMSAT = Global Mean Surface Air Temperature; SAI = Stratospheric Aerosol Injection; HiLLA = High Latitude, Low Altitude; MCB = Marine Cloud Brightening; ML = Medium-Low scenario (van Vuuren et al., 2025); PEM = Per Ensemble Member.

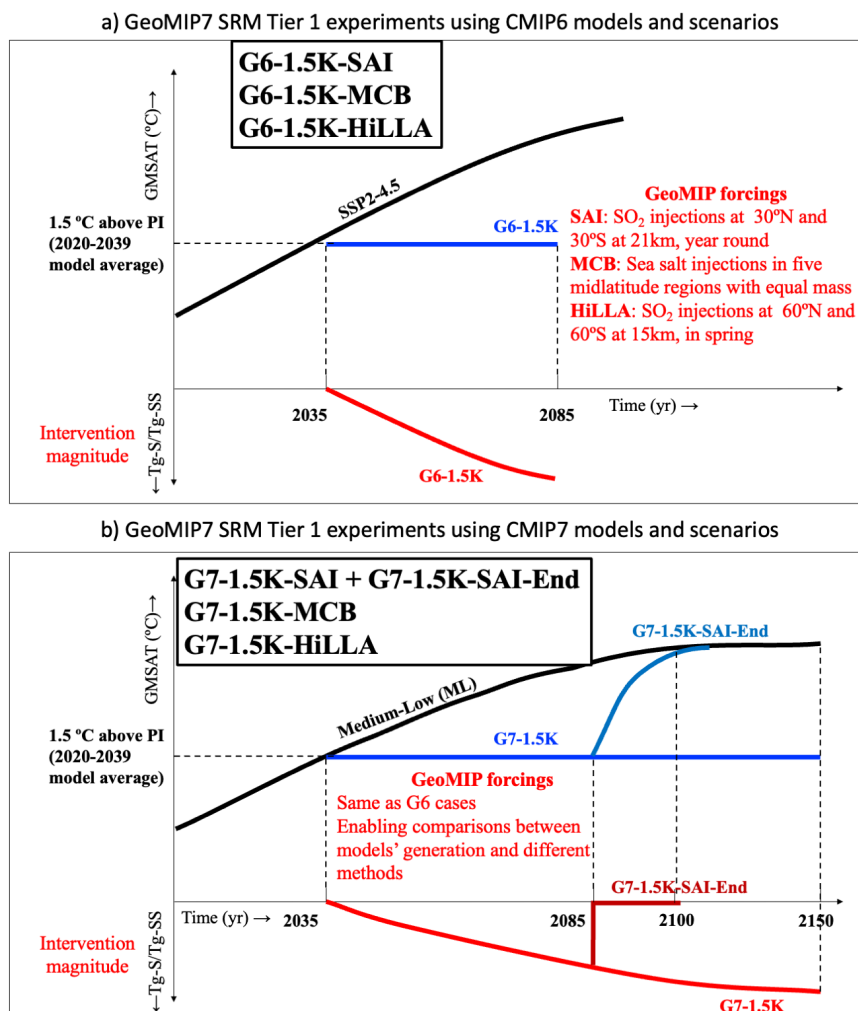
allows for models to have a consistent start date for the SRM deployment, as well as making it easier to compare across models with different base states, and across model generations.

Table 2 lists the four experiments proposed as Tier 1, together with a brief description of the intervention, that will be expanded upon in the following subsections, and details about the underlying scenario used (van Vuuren et al., 2025) and the time period in which the simulations should be run.

In terms of nomenclature, we have decided to use the G6 moniker (i.e. G6-1.5K-SAI) for simulations run with CMIP6 models and scenarios, whereas the G7 moniker (i.e. G7-1.5K-SAI) is used for simulations run with CMIP7 models and scenarios. The differences and similarities between the two scenarios are sketched in Fig. 1. For each experiment, 3 ensemble members are suggested. Considering the CMIP7 scenarios will have extensions to 2150, it will be preferable if at least one ensemble member can be extended to 2150, whereas the other are only run to 2100.

### 3.1 G7-1.5K-SAI

The G7-1.5K-SAI experiment is functionally identical to the G6-1.5K-SAI experiment, but uses a CMIP7 emissions scenario. In G7-1.5K-SAI, hemispherically symmetric SAI in the subtropical stratosphere is used to maintain a fixed GMSAT of approximately 1.5°C above the preindustrial average. The experiment branches from the ML emissions scenario, begins in model year 2035 (given how we've defined 1.5K above preindustrial, this implies the start in 2035 in all models does not require a large initial amount of SO<sub>2</sub> to be injected all at once, as it happened in the ARISE protocols for UKESM, (Henry et al., 2023))



**Figure 1.** Schematics of G6 and G7 Tier 1 experiments, with differences between underlying scenarios from CMIP6 and CMIP7 sketched and details about the forcing methodologies (consistent across G6 and G7). The black lines represent the ScenarioMIP scenarios selected as a background for the experiments; the blue lines represent the related GeoMIP experiment; the red line in the bottom part of the plots represents the intervention magnitude (depending on the specific experiment, measured in Tg-S or Tg-SS (sea salt)).

and runs until model year 2150. Each year, SO<sub>2</sub> is injected into the stratosphere in sufficient quantity to cool the planet by the amount needed to maintain the prescribed temperature target. The total quantity of SO<sub>2</sub> is placed into grid boxes at 21.5 km altitude as per the Inj-sulf-30N/S simulations above, divided evenly between 30°N and 30°S latitude.



### 3.1.1 Why symmetrical injections?

As discussed in Visioni et al. (2024), the one-degree-of-freedom (1-DOF) injection strategy used in the G6- and G7-1.5K-SAI experiments is intended to balance optimality, plausibility, and simplicity. By 1-DOF we intend that the aim of the strategy is simply to maintain GMSAT to 1.5 K, but more complexity is possible; in addition to varying the total injection quantity to manage the overall amount of global cooling. Previous research into the optimization of SAI strategy design has identified (at minimum) two more degrees of freedom in the surface temperature response (Lee et al., 2020). Firstly, an imbalance in radiative forcing between the Northern and Southern Hemispheres will push the Intertropical Convergence Zone (ITCZ) towards the warmer hemisphere; this means that single-hemisphere injection is generally considered to be undesirable (Haywood et al., 2013), and SAI simulations are usually hemispherically symmetric or strategically managed across hemispheres to maintain the interhemispheric temperature gradient. Secondly, the latitude(s) of injection determine the relative amount of cooling at the tropics vs. the poles; as such, over the past decade, strategy design has gravitated towards off-equatorial (rather than equatorial) injection to offset polar amplification and avoid overcooling the tropics and undercooling the poles. SAI simulations have been conducted which simultaneously manage, or attempt to manage, all three simultaneously (henceforth, a “3-DOF strategy”) with injections at multiple latitudes simultaneously, usually 15° and 30°N and S. However, the optimal injection strategy, or even the ideal set of injection latitudes across which to optimize, is unique to different climate models (Henry et al., 2023). To maintain the simplicity of the experiment, we instead choose a 1-DOF design (i.e., maintain GMSAT only) and choose an injection strategy likely to minimize disruption of the other two degrees of freedom. Even though hemispherically symmetrical 30° is unlikely to be the “ideal” injection strategy for any of the participating models (and, indeed, is known *not* to be for some of them), it is a reasonable choice for a 1-DOF strategy which will cool the planet while adequately cooling the poles and disrupting the ITCZ as little as possible. Analyzing how well (or poorly) the strategy achieves these secondary objectives will provide insights into how injection strategies might be improved in each model. For example, the G6-1.5K-SAI experiment overcools the Northern Hemisphere (NH) in CESM2, suggesting that Southern Hemisphere (SH) injection should be preferred in that model; however, it undercools the Arctic in UKESM1.1 and MIROC-ES2H, indicating that 30°N is not sufficiently poleward of an injection latitude to offset Arctic amplification in those models.

230

These model-dependent sensitivities are shown in Figure 2, in which the projections of zonal mean surface air temperature on the first three latitude-dependent Legendre polynomials ( $\ell_n$ ) are shown:  $T_0$  is equivalent to GMSAT ( $\ell_0=1$  indicates a pattern of AOD uniform at all latitudes),  $T_1$  represent the inter-hemispheric temperature gradient ( $\ell_1=\sin(\psi)$  indicates a pattern of AOD that is zero at the equator, and larger in one hemisphere than the other), and  $T_2$  represents the equator-to-pole temperature gradient ( $\ell_2=\frac{1}{2}(3\sin^2(\psi) - 1)$  indicates a quadratic pattern of AOD that is larger at high latitudes than at lower ones). Compared to ARISE-like simulations performed by CESM2 and UKESM (Henry et al., 2023), in which a controller algorithm (Kravitz et al., 2017) is used to determine how much sulfate mass to inject in order to maintain  $T_0$ ,  $T_1$  and  $T_2$  at 2020-2039 levels, in the G6-1.5K-SAI the symmetrical injection location leads to models responding differently in  $T_1$  (in most models, the symmetrical injection also preserves the interhemispheric temperature gradient, but not in CESM2) and  $T_2$  (in

235



240 most models, the symmetrical injection also preserves the equator-to-pole temperature gradient, but less in UKESM, also in  
ARISE, due to an increased confinement of the aerosols near the tropics due to stratospheric circulation (Bednarz et al., 2023)).  
Understanding what drives these different responses is an opportunity, rather than a drawback, for the G6-1.5K experimental  
protocol; a simple protocol enables easier investigation into the the diverging physical response in different climate models.

### 245 3.1.2 Simulations set-up

The preparatory experiments described in Table 1 are intended to assist in setting up G7-1.5K-SAI by determining the model's  
sensitivity to SAI at 30° latitude. With the sensitivity known, injection rates can be chosen to drive the climate towards, and  
maintain, the PI + 1.5°C temperature target. This could be done manually using a “guess-and-check” process, as was done in  
most models for G6sulfur (Kravitz et al., 2015); however, the process of choosing injection rates is greatly facilitated by the  
250 use of a feedback control algorithm, an approach used by some G6sulfur models and all G6-1.5K-SAI models. The preparatory  
experiments provide sufficient system identification information to write a simple feedback algorithm which can choose the  
required injection rates in the presence of uncertainty in the response and variability. This process was first used to design a  
3-DOF experiment by MacMartin et al. (2017) and Kravitz et al. (2017); while the design process for the original feedback  
algorithm was quite complex, it is possible to modify their original algorithm for similar 3-DOF and 1-DOF experiments quite  
255 easily. The necessary unknowns are constants, called controller gains, which determine how much SO<sub>2</sub> to inject based on the  
running deviation from the temperature target. A process for deriving these gains from the original algorithm is described by  
Lee et al. (2025a) in their Section 2.2, but to briefly summarize: if the sensitivity of a climate model (in units of °C per Tg/SO<sub>2</sub>  
per year) to 30°N + 30°S injection is known, adequate controller gains for controlling GMSAT with SAI at 30°N + 30°S can be  
computed, producing a gain in units of [Tg/SO<sub>2</sub> per year][°C<sup>-1</sup>]. This gain can then be used to construct a feedback algorithm  
260 in the form of Eq. 1 in Lee et al. (2025a).

Models that do not have interactive stratospheric aerosols can still run G7-1.5K-SAI: they can either use their own strato-  
spheric aerosol distribution (as done by both MPI versions in the G6sulfur experiments, and by CNRM (Vioni et al., 2021b)),  
as long as it looks reasonably symmetrical between the hemispheres, or they can use a scaled version of the CESM2-WACCM6  
265 generated distribution (or other models) for the G6-1.5K-SAI, as proposed in the Climate Chemistry Model Intercomparison  
CCMI-2022 senD2-sai experiment (Tilmes et al., 2025), to fully simulate the aerosol impacts in the stratosphere. In the latter  
case, modeling centers can request a data set of aerosol radiative properties (extinction coefficient, single-scattering albedo,  
asymmetry factor) on their model-specific wavelengths. Such data will be provided on request – as modeling centers will also  
have to share the details of their short-wave and long-wave radiative transfer model spectral grids – and prepared with the  
270 RETrieval Method for optical and physical Aerosol Properties in the stratosphere (REMAPv1) that was described in Jörmann  
et al. (2025). In short, the REMAPv1 method works by first retrieving the parameters of a single-mode log-normal aerosol  
size distribution that represents the input dataset in a best-fit sense. From there, it computes optical properties on any specified  
wavelengths (or wavelength bands) using Mie theory. In this manner, using REMAPv1, modeling centers can also obtain all

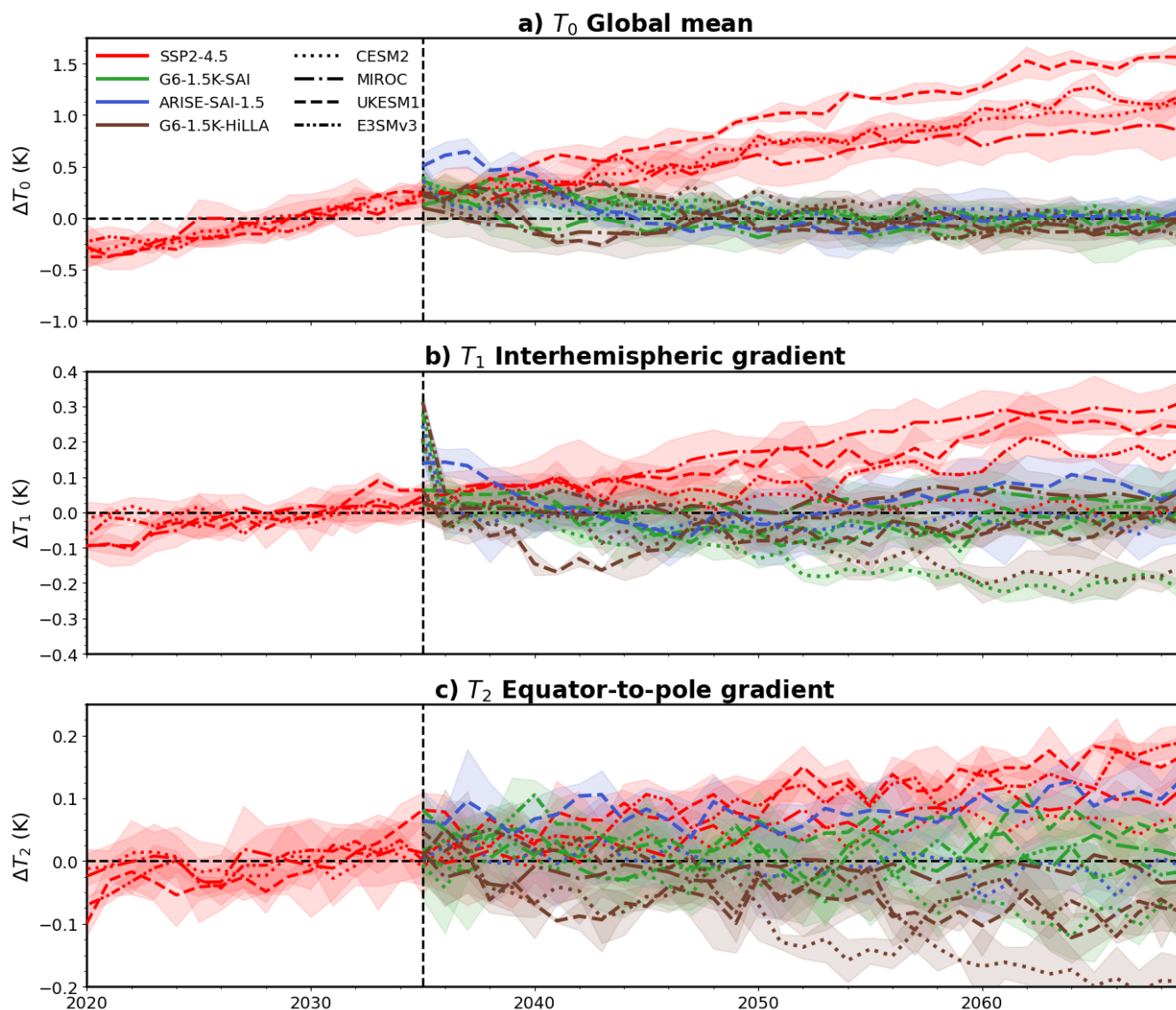


**Figure 2.** Evolution of a) global-mean temperature  $T_0$ , b) interhemispheric temperature gradient  $T_1$ , and c) equator-to-pole temperature gradient  $T_2$  from 2020-2069 for SSP2-4.5 (red) and SAI scenarios (G6-1.5K-SAI, green; ARISE-SAI-1.5, blue; HiLLA-SAI, brown). Line style denotes the climate model (CESM, MIROC, UKESM and E3SM) and line shading show the ensemble spread.

necessary aerosol properties from the preparatory Inj-sulf cases described in Section 2 from other models to understand their own model's climate response to different patterns of aerosols.

275



### 3.2 G7-1.5K-SAI-End

Many members of the community have highlighted the importance of conducting a coordinated experiment that includes an abrupt termination of SAI (Parker and Irvine, 2018) in the context of GeoMIP. Robock et al. (2008) first included an abrupt termination in their SAI experiment using constant yearly emissions of SO<sub>2</sub>. A similar experiment was then part of the original G4 experiment (Kravitz et al., 2011), and the climatic responses were then explored in multiple papers (Trisos et al., 2018; Jones et al., 2013); it has now been deemed to be an important inclusion in the CMIP7 simulations in order to offer a more comprehensive picture of potential SAI risks. For this reason, we propose a G7-1.5K-SAI-End experiment that branches off from the G7-1.5K-SAI, abruptly ending SO<sub>2</sub> injections at the end of 2084, and that continues simulations for at least 15 years to understand Earth system responses under an abrupt warming. Simulations with an abrupt termination can also be leveraged to emulate the response under more moderate phase-outs scenarios by expanding the scenario space (Farley et al., 2024), and are also likely to inform assessment of SAI impacts on tipping dynamics and risks therein (Zhao et al., 2025; Lenton et al., 2025; Bednarz et al., 2025a).

### 3.3 G7-1.5K-HiLLA

As with G7-1.5K-SAI and G6-1.5K-SAI, the G7-1.5K-HiLLA (“High-Latitude, Low-Altitude”) experiment is identical to the earlier G6-1.5K-HiLLA experiment (Duffey et al., 2026), except that it uses the CMIP7 emissions scenario. G7-1.5K-HiLLA matches the global mean temperature target of G7-1.5K-SAI, but instead of year-round subtropical (30°) injection, the G7-1.5K-HiLLA experiment uses spring/early-summer (MAMJ for the NH, SOND for the SH) low-altitude (15 km) injection in the sub-polar latitudes (60°). This is a scenario which aims to represent a plausible early-stage, logistically constrained deployment of SAI (Wheeler et al., 2025), that might be deployable using modified existing aircraft, rather than using novel high-flying ones (Duffey et al., 2025). Unlike for G7-1.5K-SAI, the longitude of injection is prescribed, at 180° E. With lower altitude injection, longitude likely has larger effects than at high altitudes (Sun et al., 2023), and previous HiLLA simulations show non-negligible impacts of varying longitude, particularly in the Southern Hemisphere (Duffey et al., 2026).

Hemispherically symmetric injections are used in the G7-1.5K-HiLLA scenario for the same reasons as the G7-1.5K-SAI case above. As above, this strategy will not perfectly maintain interhemispheric temperature gradient in any model, and there is substantial divergence across models in the zonal mean temperature response under G6-1.5K-HiLLA (Figure 4), in part due to differences in the model’s Arctic amplification in the background SSP2-4.5 warming. In UKESM1-1 and MIROC-ES2H, the substantial high latitude NH residual warming present under G6-1.5K-SAI is reduced under G6-1.5K-HiLLA. Alternatively, overcooling in the NH high latitudes in CESM2-WACCM under G6-1.5K-SAI is increased even further under G6-1.5K-HiLLA.

#### 3.3.1 Why 15 km injection altitudes?

Testbed simulations (Duffey et al., 2026) indicated a strong dependence on injection altitude under HiLLA strategies, with global mean cooling increased from 0.6°C per 12 Tg SO<sub>2</sub> to 1.0°C per 12 Tg SO<sub>2</sub>, when altitude is increased from 13 km to



15 km. The maximum altitude of various large jetliners is 13 km (Smith et al., 2024), so the G6-1.5K-HiLLA strategy may not  
310 represent a logistically feasible strategy with these aircraft. However, given the significant global cooling required to meet the  
G7-1.5K strategy, and so produce a climate state comparable with G6-1.5K-SAI, the altitude of 15 km was chosen to achieve  
sufficient cooling efficiency to prevent the need for extremely large injection magnitudes.

### 3.3.2 Simulations set-up

The experimental setup for G7-1.5K-HiLLA is identical to that of G7-1.5K-SAI, except that 15 km springtime 60° injection  
315 is used instead of 21.5 km year-round 30° injection. Once the model sensitivity to 60° injection is known, the injection rates  
can be determined through the same process outlined in Section 3.1.2. Across the four models with simulations of both G6-  
1.5K-HiLLA and G6-1.5K-SAI, the relative global mean cooling efficiency,  $\frac{E_{\text{HiLLA}}}{E_{\text{SAI}}}$  (where E is global mean cooling per unit  
injection), ranges from 0.57 to 0.64 K/Tg-S across the four models (0.57 in CESM2-WACCM, 0.64 in UKESM1-1, 0.64 in  
E3SMv3, and 0.60 in MIROC-ES2H). Equivalently, G6-1.5K-HiLLA requires 1.56 to 1.76 times the injection magnitude of  
320 G6-1.5-SAI to achieve the same target state. Given that injection occurs in only four months in each hemisphere, the rate of  
SO<sub>2</sub> injection in G6-1.5K-HiLLA is approximately five times higher than that under G6-1.5K-SAI. HiLLA strategies achieve  
their global mean cooling via greater polar and less tropical cooling than low latitude injection strategies (Figure 4), and so the  
HiLLA efficiency would be reduced if defined in terms of the cooling of low latitude regions Duffey et al. (2026).

### 3.4 G7-1.5K-MCB

325 The G7-1.5K-MCB experiment follows the choices made for the G7-1.5K-SAI experiment, except that it uses MCB, and is  
functionally identical to G6-1.5K-MCB (Hirasawa et al., 2025a) but using the CMIP7 ML emission scenario as its reference.  
In G7-1.5K-MCB, MCB is applied by increasing injected sea salt aerosol emissions in the lowest model layer of grid cells with  
ocean fraction greater than 0.5 in five midlatitude ocean areas : the North Pacific (NP: 30°N to 50°N and 190°W to 120°W),  
North Atlantic (NA: 30°N to 50°N and 70°W to 0°W), South Pacific (SP: 50°S to 30°S and 170°W to 90°W), South Atlantic  
330 (SA: 50°S to 30°S and 55°W to 15°E), and South Indian Ocean (SI: 50°S to 30°S and 30°E to 100°W). The total mass of  
emissions are set to be equal in both hemispheres and at a constant emission rate throughout a given year. MCB is used to  
maintain GMSAT within  $\pm 0.2^\circ\text{C}$  of  $1.5^\circ\text{C}$  above the preindustrial average by increasing emissions over time to cool global  
mean surface temperatures to this level. The experiment branches from the ML emissions scenario at model year 2035, and  
runs until model year 2150.

#### 335 3.4.1 Why hemispherically mass-balanced injections?

Similar to G7-1.5K-SAI, the MCB equivalent is designed as a one degree-of-freedom strategy that strikes a balance between  
achieving a climate response that reasonably offsets the greenhouse gas warming effect and remaining simple enough to be im-  
plemented by a range of state-of-the-art ESMs (Hirasawa et al., 2025a). Exploratory analysis in three CMIP6 ESMs (Hirasawa  
et al., 2026) found that emitting sea salt aerosol into five mid-latitude regions (NP, NA, SP, SA, SI) resulted in temperature and



340 precipitation response patterns that were more spatially uniform, and thus more closely matched the GHG signal, than previously explored MCB strategies that focused on emissions in lower latitude regions (Stjern et al., 2018; Haywood et al., 2023; Lee et al., 2025a). Specifically, shifting emission to higher latitudes reduces the tropical overcooling signal associated with 30°S to 30°N emissions used in previous GeoMIP simulations (Kravitz et al., 2013; Stjern et al., 2018) and the La Niña-like cooling signal characteristic of protocols that focused on the tropical Pacific (Jones et al., 2009; Rasch et al., 2009; Haywood et al., 2023; Rasch et al., 2024; Odoulami et al., 2024; Lee et al., 2025a). Following from this, we further define the emission rates in each region such that the areal-sum emissions are 1/4th of the total emissions in each of the two Northern Hemisphere regions (NA and NP) and 1/6th of the total emissions in each of the three Southern Hemisphere regions (SP, SA, and SI) to minimize shifts in ITCZ by distributing the perturbation evenly across the hemispheres.

While hemisphere-symmetric midlatitude MCB emission simulations demonstrate substantial improvements over past protocols, it is unlikely to be an optimal distribution for returning climate to early-21st century conditions (Fig. 3d,f). Considering the distinct response patterns for MCB in different regions (Hirasawa et al., 2026), further optimization is feasible (Mason et al., 2025). However, the optimal MCB emission distribution will differ across models due to differences in aerosol-cloud interactions (giving rise to different regional forcing strengths) and atmosphere-ocean circulation and climate feedbacks (giving rise to different patterns of climate response under global warming and under MCB). For G6-1.5K-MCB, UKESM1.1 and MIROC-ES2H show Arctic under-cooling, which indicates MCB in an additional region at polar latitudes may be required in these models (Mason et al., 2025; Henry et al., 2025). CESM2 shows NH cooling relative to the SH while E3SMv2 shows NH warming relative to the SH, which suggests additional MCB should be applied in the Southern hemisphere in CESM2 and in the NH in E3SMv2. Furthermore, CESM2 simulations that balanced the sea salt mass emissions to produce equal forcing in each hemisphere produced excessive NH cooling and southward shifts in the ITCZ (Hirasawa et al., 2025a). These variations across models demonstrate that there is not a single emission distribution that would maintain the hemispheric asymmetry consistently across all models and that forcing is not necessarily a good predictor of hemispheric temperature response due to differences in radiative feedbacks and circulation response. Thus, to maintain simplicity in model configuration and to ease the interpretation of inter-model differences, we select mid-latitude MCB with mass emissions distributed evenly between the NH and SH as the basis of a 1-DOF design as a first-order attempt to reduce inter-hemispheric asymmetries.

### 365 3.4.2 Simulations set-up

The Inj-seasalt-midlat experiment described in Table 1 and section 2.2 is designed to determine a given model's sensitivity to mid-latitude MCB, which can be used to set up G7-1.5K-MCB. With this sensitivity known, the sea salt aerosol injection rates can be chosen to maintain the GMST target. This can be done by adjusting emissions manually over the simulation period ("guess-and-check") or by using a feedback controller algorithm. Inj-seasalt-midlat provides information on the magnitude and time scale of the cooling response to mid-latitude MCB at a given emission rate, which are the two key pieces of information for computing the parameters of a 1-DOF feedback controller (see appendix A of Hirasawa et al. (2025a)). The time scale of climate response to MCB tends to be longer than the response to SAI, thus the feedback gains required for a G7-1.5K-MCB controller may differ from those used in a G7-1.5K-SAI controller. The MCB forcing is inherently non-linear, due to the sub-



375 linear behaviour of aerosol activation (Rasch et al., 2024). This makes it challenging to estimate a full MCB emission time series prior to running a scenario simulation (also known as a "feedforward" estimate), because the model sensitivity derived from Inj-seasalt-midlat will be an underestimate early on in the simulation, when emissions are still low, and an overestimate late in the simulation, when clouds become saturated with aerosol. Feedback controllers can partially account for such nonlinearities, as they can adjust emissions in response to these deviations.

### 3.4.3 Alternate CDNC set-up

380 While we expect that most CMIP7 generation ESMs will be capable of increasing accumulation mode sea salt aerosol, some may have limitations that prevent adequate representation of G7-1.5K-MCB with sea salt aerosol emissions. For such models, it may be more practical to directly perturb the cloud droplet number concentration (CDNC) in the five midlatitude MCB regions (see Hirasawa et al. (2025a) section 2.4 for simulation descriptions). CDNC perturbations have been used in several past MCB simulation protocols (Rasch et al., 2009; Kravitz et al., 2013; Hirasawa et al., 2023; Chen et al., 2025; Lee et al., 2025a) and  
385 we expect that sea salt aerosol injection and CDNC perturbation simulations will produce similar climate responses, if they produce the same radiative forcing Rasch et al. (2024). Nevertheless, this method is idealized and neglects key processes like aerosol activation, aerosol transport, and aerosol direct forcing, potentially underestimating the inter-model uncertainty. Thus, we recommend using sea salt aerosol emissions when possible.

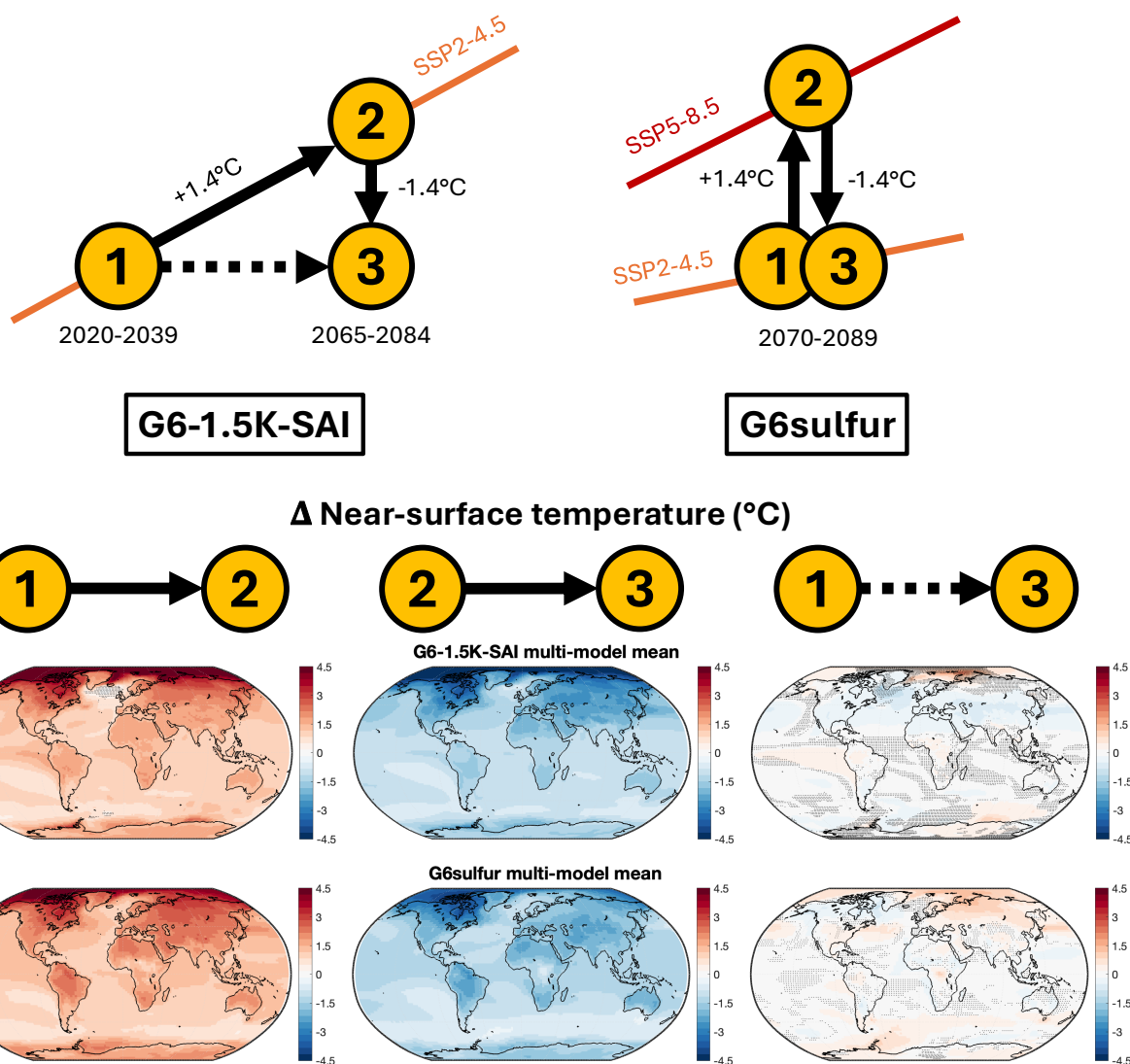


**Figure 3.** From Lee et al. (2026b): Maps of near-surface air temperature changes (in °C) for G6-1.5K-SAI and G6sulfur, between three different periods: (1) the reference period, corresponding to the period over which the GMSAT targets are defined; (2) the warmed world; and (3) the new climate state reached under GHG plus SAI. The left column plots the difference between (1) and (2), representing the impacts of global warming alone; the middle column plots the difference between (2) and (3), representing the impacts of SAI alone; and the right side column plots the difference between (1) and (3), representing the combined impacts of warming and SAI. For G6-1.5K-SAI, period (1) is SSP2-4.5 2020-2039, period (2) is SSP2-4.5 2065-2084, and period (3) is G6-1.5K-SAI 2065-2084. For G6sulfur, all three periods are averages of 2070-2089 data, in which the amount of cooling is approximately the same (1.4°C) as the last 20 years of G6-1.5K-SAI. Shading represents areas where models disagree on the sign of the change (fewer than 3 out of 4 for G6-1.5K-SAI, and fewer than 4 out of 6 for G6sulfur).

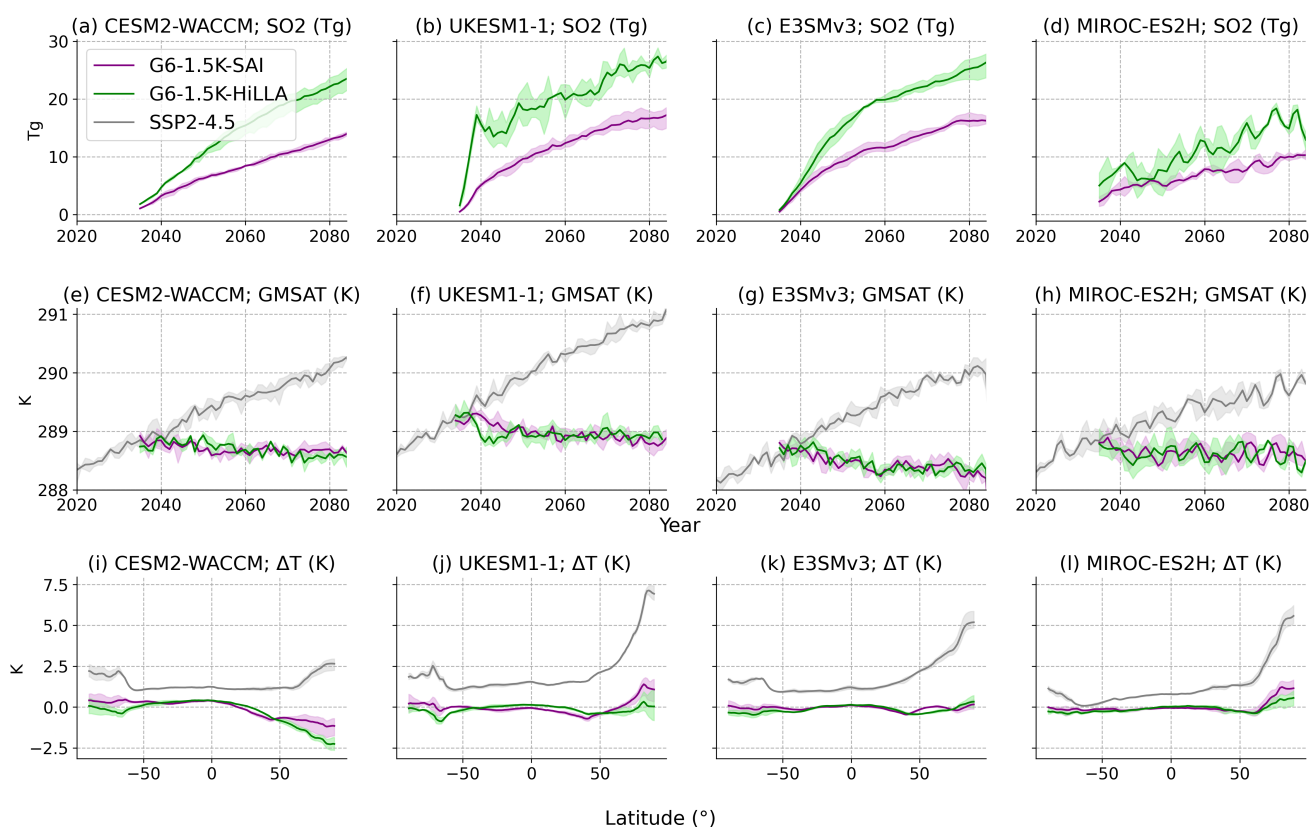


**Figure 4.** (a-d) Injection magnitude (Tg SO<sub>2</sub>), (e-h) Global mean surface air temperature (GMSAT), and (i-l) zonal mean temperature change relative to the 2020-2039 baseline ( $\Delta T$ ), for the four models with G6-1.5K-SAI and G6-1.5K-HiLLA simulations. The solid lines show ensemble means and shaded areas show ensemble range, using the first three members for all scenarios.

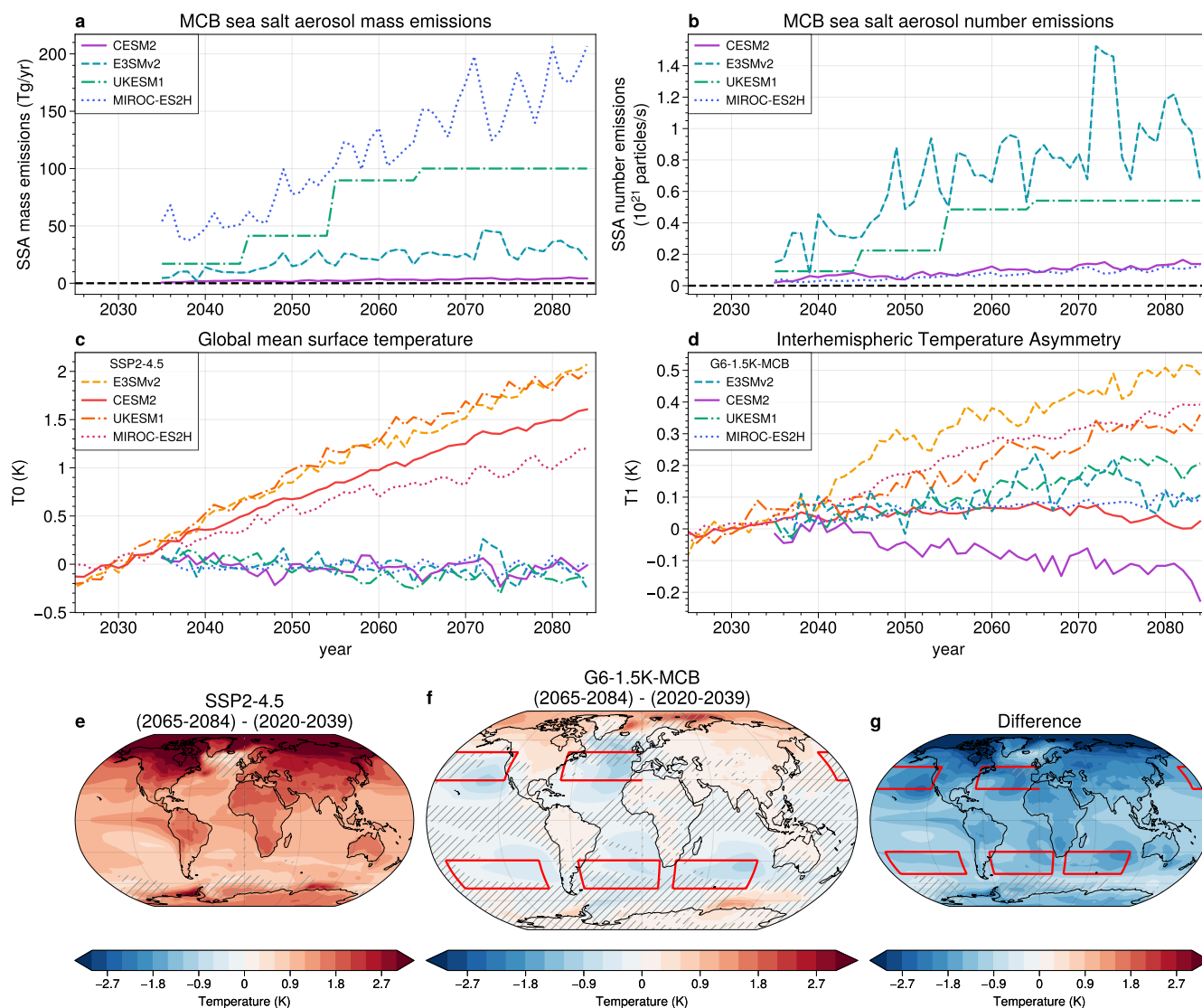


**Figure 5.** Results of G6-1.5K-MCB simulations in four ESMs (E3SMv2.0, CESM2.1, UKESM1.0, and MIROC-ES2H). Top row shows the sea salt mass flux (a) and number flux (b) required in each model to maintain the 1.5K GMST target. Middle row shows the T0 (c) and T1 (d) time series for the SSP2-4.5 reference simulations (red shades) and G6-1.5K-MCB simulations (blue shades). Bottom row shows the spatial pattern of annual mean reference height (2m) temperature anomalies averaged across the models for SSP2-4.5 (e), G6-1.5K-MCB (f), and the difference between the two (g) (the MCB effect). Hatching indicates grid points where at least one model disagrees on the sign of the response.



Experiment name	Description of intervention	Underlying emission scenario	Period
G7-1.5K-SAI-Late	Delay of the G7-1.5K-SAI scenario with a start in 2055	ML	2055-2100
G7-1.5K-SAI-LN	Equal yearly injections of SO <sub>2</sub> at 30°N and 30°S to maintain GMSAT at 1.5°C above PI	LN	2035-2150
G7-0.5K-SAI	Equal yearly injections of SO <sub>2</sub> at 30°N and 30°S to maintain GMSAT 1.0°C colder than G7-1.5K-SAI	ML	2035-2150

**Table 3.** Scenario exploration Tier 2 experiments. GMSAT = Global Mean Surface Air Temperature; SAI = Stratospheric Aerosol Injection; ML = Medium-Low scenario (van Vuuren et al., 2025); LN = Low-to-Negative scenario. As we don't expect all modeling teams to perform these experiments, and they are not comprehensive nor prescriptive, no total amount of years of simulation is provided.

#### 4 Tier 2 experiments

390 Over time, different modeling groups have devised their own specific SRM experiments, either selecting different scenarios and targets, or proposing new methods or deployment strategies, based on different interests and needs; it is neither possible nor advisable to claim each one of them should be an official GeoMIP experiment. However, it was suggested during the last few GeoMIP meetings to have a central space to collect ideas and identify other groups interested. Therefore, in this section we collect a series of lower priority experiments that can be run in order to enrich the analyses from the Tier 1 experiments.

395 Considering the potential infinite space of experiments, it will be important for modeling teams and research groups to communicate promptly about what experiments they are running so that an up-to-date registry of ongoing Tier 2 experiments can be kept on the GeoMIP website, similarly to what was proposed in Kravitz et al. (2015) for test-bed experiments. This may be useful, for example, to generate spin off working groups focused on mechanistic investigation to further inform interpretation of Tier 1 simulations. In general Tier 2 simulations can be categorized as scenario exploration, SRM strategy exploration, and

400 process level understanding, and will be discussed in turn below.

##### 4.1 Tier 2 experiments exploring different scenarios

This set of experiments is meant to extend exploration of scenarios through the inclusion of different amounts of cooling (G7-0.5K-SAI), a different underlying scenario (G7-1.5K-SAI-LN), or the exploration of a delayed start (G7-1.5K-SAI-Late). These scenarios are shown in Fig. 6. This set is not meant to be comprehensive, but rather to suggest the capacity to run further

405 experiments with scenarios of interest.

The importance of considering a larger range of scenarios, including both higher or lower cooling targets and the inclusion of changes in the deployment (i.e. interruptions, phase-outs) has been highlighted before (MacMartin et al., 2022). While this space is potentially infinite, and highly dependent on the assumptions of the underlying emission scenario (Baur et al., 2023),

410 there is clearly merit in both considering different degrees of cooling (Visioni et al., 2023b), as well as potential inconsistencies



Tier 2 experiments compared to G7-1.5K-SAI

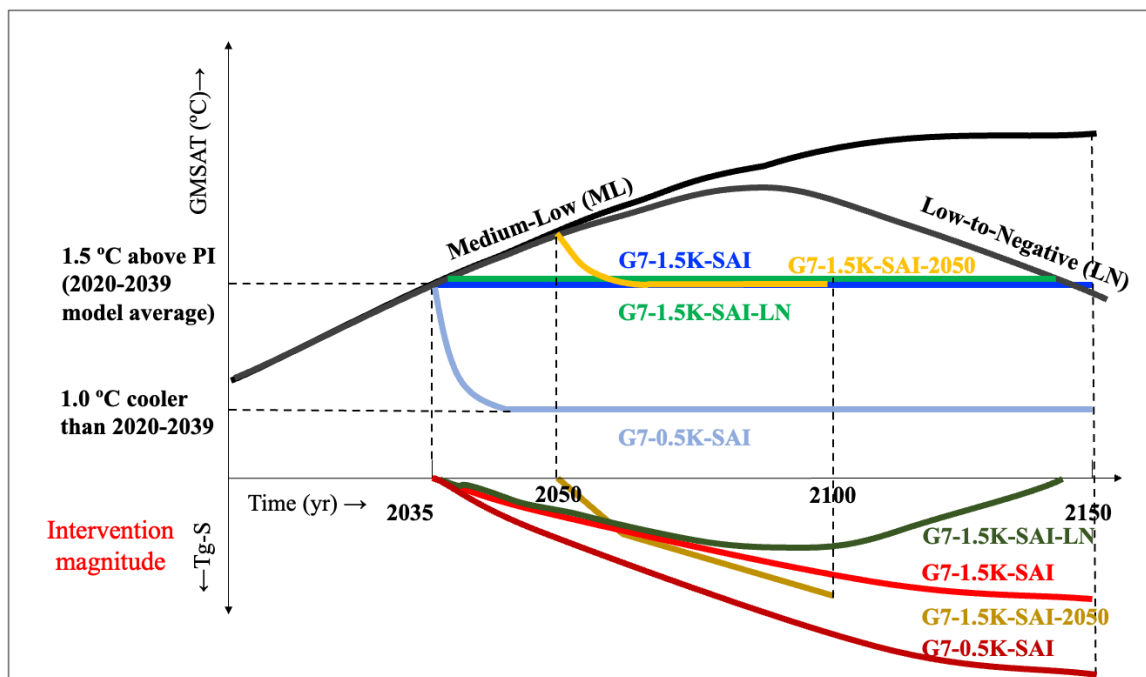


**Figure 6.** Schematics of Tier 2 scenario exploration experiments for the SAI case, with the inclusion of main Tier 1 scenario (G7-1.5K-SAI) for comparison

in deployment (Farley et al., 2024), and the results of such broader set of simulations can also be included in emulators that already integrate GeoMIP data (Martínez Montero et al., 2022; Muñoz-Sánchez et al., 2025; Farley et al., 2026). Here we provide some suggestions of how such an expanded exploration could look, leaving some choice to modeling groups with different interests to expand on this, as long as some coherence through the common simulation of Tier 1 experiments is maintained, as was done previously (Tilmes et al., 2020; Baur et al., 2025).

**G7-0.5K-SAI** a potential case cooling 1 K more than the G7-1.5K-SAI case, which would lead to a higher rate of deployment, and which could be compared against the 1.5 K to understand trade-offs between more cooling and other relevant surface climate impacts such as air quality impacts (Wang et al., 2026) and agricultural impacts (Clark et al., 2023), as well as to investigate the efficacy of SRM strategies to reduce climate risk including risks associated with tipping elements against the backdrop of a greater masking of GHG induced warming. The larger injection needed to cool by that amount should be ramped up linearly over the first 10 years as done in the ARISE-SAI-1.0 case (Brody et al., 2024).



**G7-1.5K-SAI-LN** a potential case could explore having the same cooling target as G7-1.5K-SAI, but on a lower (LN) or higher (M) underlying emission scenario, to look at different impacts under different scenarios, as proposed in the test-bed experiments described in Tilmes et al. (2020) using the SSP5-3.4OS temporary overshoot experiment.

425 **G7-1.5K-SAI-Late** some studies have recently explored the differential impacts of an SAI deployment depending on the starting date, highlighting differences in ocean heat uptake and stratospheric ozone changes due to different chlorine loads in the stratosphere (Brody et al., 2024; Pfüger et al., 2024). This type of experiment is further motivated by calls to understand the ability of SAI to reverse GHG driven changes to drivers of climate tipping in the cryosphere, biosphere, ocean and atmosphere, which include the deceleration of AMOC (Pfüger et al., 2024), melting of glaciers and permafrost, and risk of amazon dieback, among others (Lenton et al., 2025). Delayed implementation studies may support greater understanding of what SAI can and cannot do as a function of the timing of deployment during this century. For a GeoMIP experiment, we propose a delay of 15 years compared to the start of G7-1.5K-SAI, and to run the experiment for at least 50 years.

This potential set of experiments, in a multi-model context, would be extremely useful when thinking about the broader context of emission trajectories, temporary overshoot dynamics and climate stabilization more broadly (Palazzo Corner et al., 2023); the comparison of experiments with different underlying emission scenarios, and/or between different cooling targets, can shed light on how SRM would impact carbon cycle dynamics (Zhao et al., 2024) (considering the emission-driven pathways in CMIP7 models (Meinshausen et al., 2024)), and how it compares to net-zero and negative emission scenarios using Carbon Dioxide Removal (CDR) (Sanderson et al., 2025); as well as feed into discussions of the reversibility or irreversibility of specific climatic changes, and of tipping elements dynamics in the context of SRM (Hirasawa et al., 2023; Zhao et al., 2025; Lenton et al., 2025), especially as it pertains to different degrees of warming, or timing, at which climate stabilization may occur (Winkelmann et al., 2025; Pfüger et al., 2024).



Experiment name	Description of intervention	Underlying emission scenario	Period
G7-1.5K-MCB-2DOF	Injections of sea salt aerosols in five midlatitude regions with different mass across hemispheres to maintain GMSAT and $T_1$ gradient at 1.5°C above PI	ML	2035-2150
G7-1.5K-SAI-3DOF	Yearly injections of SO <sub>2</sub> at 30°N, 15°N, 15°S and 30°S in different amounts to maintain GMSAT, $T_1$ and $T_2$ gradients at 1.5°C above PI	ML	2035-2150
G7-1.5K-SAI-Solid	Yearly injections of solid particles (CaCO <sub>3</sub> , Al <sub>2</sub> O <sub>3</sub> ) at 30°N and 30°S to maintain GMSAT at 1.5°C above PI (mass manually adjusted every decade)	ML	2035-2150
G7-1.5K-Shade	A case of G7-1.5K performed through uniform reduction of the solar constant at the top of the atmosphere	ML	2035-2150
Inj-seasalt-polar	Injection of sea salt aerosol in ice-free ocean regions at 60-80°S in austral summer (DJFM) and 60-80°N in boreal summer (JJAS) to maintain polar (70-90°N/S) temperatures at their 2020-39 levels	ML	2035-2085

**Table 4.** Strategies exploration Tier 2 experiments. GMSAT = Global Mean Surface Air Temperature; SAI = Stratospheric Aerosol Injection; DOF = Degrees of Freedom; MCB = Marine Cloud Brightening; ML = Medium-Low scenario (van Vuuren et al., 2025). As we do not expect all modeling teams to perform these experiments, and they are not comprehensive nor prescriptive, no cumulative sum for the years of simulation for all experiments is provided.

## 4.2 Tier 2 experiments exploring different SRM strategies

Together with an exploration of different scenarios as discussed in the previous section, there is significant interest in coordinating simulations for other SRM strategies. These include variations on SAI and MCB to explore the influence of intervention location and material, as well as process-oriented inter-comparisons of other SRM proposals. Here, we outline several experiments based on previous and ongoing modeling work. This list is not comprehensive and we encourage groups to explore the scenario and strategy space.

A non-comprehensive set of potential experiments is provided in Table 4, and might include:

**G7-1.5K-MCB-2DOF** : Climate model analyses have pointed out the importance of minimizing inter-hemispheric temperature gradients, as single-hemisphere MCB perturbations can cause dramatic shifts in tropical precipitation (Emme et al., 2025). Modeling groups may therefore consider an iteration on the G7-1.5K-MCB in which the areal-sum emission rate in each hemisphere is adjusted to manage two degrees of freedom (2DOF) - the GMSAT and the inter-hemispheric temperature gradient ( $T_1$ ). This may require additional preparatory experiments in which MCB emissions are applied in each hemisphere independently for the reasons described at the end of section 3.4.1. While a 3DOF case aligning with SAI may enable clearer inter-method comparison, more research on polar-latitude MCB would be required to determine if the equator-to-pole gradient can also be controlled.



**G7-1.5K-SAI-3DOF** : Modeling groups interested in developing more comprehensive, targeted simulations of SAI by better understanding the design space of SAI in their model, should consider running a case of G7-1.5K-SAI trying to manage 3 degrees of freedom (DOFs), using the same protocol as ARISE-SAI (Richter et al., 2022). This is a more complex injection protocol than G7-1.5K-SAI, but is designed to yield smaller regional temperature differentials relative to the target period. In this protocol, GMSAT, interhemispheric temperature gradient, and equator-to-pole temperature gradient (referred to as  $T_0$ ,  $T_1$ , and  $T_2$ , respectively, by Richter et al., 2022) are simultaneously maintained at  $PI+1.5^\circ C$  (2020-2039) levels. This is accomplished with injections in independent amounts at  $30^\circ N$ ,  $15^\circ N$ ,  $15^\circ S$ , and  $30^\circ S$ , with injection rates chosen based on the various Inj-sulf preparatory experiments described in 2.

**G7-1.5K-SAI-Solid** : Stratospheric heating through the absorption of (mainly) terrestrial radiation by sulfate aerosols not only affects stratospheric climate, but also surface climate, as demonstrated in Wunderlin et al. (2024); Simpson et al. (2019); Visioni et al. (2021a). To minimize stratospheric heating, several studies have proposed alternative, solid materials for stratospheric aerosol injections (e.g., Dykema et al., 2016; Vattioni et al., 2024a, and references therein). In a single-model study Stefanetti et al. (2024) have found calcite, alumina, and diamond nano-particles to alleviate absorptive heating, while the latter also results in a greater surface cooling efficiency, i.e. requiring smaller injection masses for a given temperature target. Ozone changes could also be reduced through the use of solid particles, although substantial uncertainties remain around the actual chemistry impacts of materials not usually found in the stratosphere (Vattioni et al., 2023, 2025). To improve the robustness of solid aerosol injection modelling, some modellers perform activities within SolidMIP, an active community under the GeoMIP umbrella, focused on the intercomparison of model development work around solid particle SAI and uncertainties in physico-chemical and optical properties of various alternative materials. Within SolidMIP some modeling centers are working towards a case of G7-1.5K-SAI using solid particles instead of sulfate precursors, to lay the groundwork for a future coordinated multi-model approach involving more groups. G7-1.5K-SAI-Solid will consist of two simulations in addition to G7-1.5K-SAI, one for each proposed solid material: calcite ( $CaCO_3$ ) and alumina ( $Al_2O_3$ ). Even though Stefanetti et al. (2024) also considered diamond (C(diam)) nanoparticles, which showed the best cooling efficiency and least side-effects, we omit it here because of the recent findings showing that actual industrial diamonds have hybridized impurities substantially deteriorating its optical properties (Kumar et al., 2026). Simulations with the remaining two solid aerosol particle types will be performed in one or more models with full microphysical and radiative treatment of the stratospheric solid aerosol. The injection amount in these preparatory simulations will be manually adjusted to maintain the 1.5 K temperature target, with models' response provided in similar experiments as those proposed in Section 2 for the Inj-Sulf-30N/S cases but using fixed amounts of solid particles. The resulting forcing from G7-1.5K-SAI-Solid will then be provided to the community and can be tailored to each individual model as required using the forward Mie calculation part of REMAPv1 (Jörmann et al., 2025). The introduction of the same forcing into different models will provide a range of temperature responses both at the surface and in the atmosphere that can be analyzed as a first step. While extremely important to capture the whole balance of potential



impacts from solid particles injections, detailed chemical effects will not be included in this first set of simulations for simplicity, and due to the larger uncertainties for those materials (Vattioni et al., 2025).

495 **Inj-seasalt-polar** : Henry et al. (2025) performed Arctic MCB cooling simulations with sea salt emissions between 60°N and 80°N where there is no land or sea ice in a sub-set of models used for G6-1.5K-MCB (Hirasawa et al., 2025a). Arctic MCB successfully maintained Arctic mean temperatures and the models suggested there were few significant lower-latitude precipitation impacts, in contrast to single-hemisphere high latitude SAI (Lee et al., 2023). In one model (UKESM1), it was found that there is an upper limit on the possible cooling in the Arctic by MCB (Henry et al., 2025), suggesting a larger inter-model comparison of sensitivity experiments is warranted. We suggest an idealized polar MCB  
500 case with sea salt aerosol emissions in ice-free ocean regions between 60° and 80° in both hemispheres during the summer months when insolation is the highest (JJAS in the NH and DJFM in the SH) with step emissions following the preparatory experiment protocols in Table 1.

**G7-1.5K-Shade** : Modeling groups interested in diagnosing and separating the aerosols-driven changes on surface climate should consider running an experiment similar to G6solar, in which the same temperature target is achieved through a  
505 uniform reduction of incoming solar radiation at the top of the model. This has proven beneficial in highlighting aerosols-driven uncertainties (Visoni et al., 2021b). Furthermore, these simulations would prove beneficial in understanding the impacts of potential space sunshades (Fuglesang and de Herreros Miciano, 2021).

**Combination and contrast of SRM methods and other techniques** : There is increasing discussion and opportunity to think of experiments that include a potential "cocktail" of different SRM techniques (Cao et al., 2017), such as for MCB  
510 combined with SAI. Future work could explore and define a protocol for such experiments, which we do not yet propose here currently. Similarly, there should be the opportunity to explore the combination of some SRM techniques with other climate intervention proposals that fall more within the realm of changes in atmospheric composition, such as CO<sub>2</sub> removal (Clark et al., 2025) or methane removal (Li et al., 2023), or localized albedo modification techniques (Moore et al., 2021), in order to understand potential synergies as well as unforeseen negative interactions between  
515 them. Simulations that achieve the same temperature target as G7-1.5K with carbon or methane removal alone can also be useful to understand differences in the surface climate responses across intervention types (Laakso et al., 2020).



Experiment name	Description of intervention	Underlying emission scenario	Period
MCT-L1-Background	Scale down the control background INP	fixed SST	min 10 years
MCT-L1-Seeding	Spatially uniform addition to the background INP	fixed SST	min 10 years

**Table 5.** MCT-L1 Tier 2 experiments. MCT = Mixed-phase Cloud Thinning; INP = Ice-Nucleating Particles; SST = Sea-Surface Temperature. Both configurations are atmosphere-only and perturb the INP concentration used for heterogeneous freezing (see §4.3 for the full protocol and Table 7 for the detailed simulation matrix).

### 4.3 Mixed-Phase Cloud Thinning experiments

Besides the combination of SAI and MCB discussed in the previous section, another promising approach to polar climate intervention is Mixed-Phase Cloud Thinning (MCT). MCT is a proposed radiation modification method that exploits the thermodynamic instability of mixed-phase clouds — clouds containing supercooled liquid droplets coexisting with ice crystals at temperatures between approximately 0 and  $-39^{\circ}\text{C}$ . By seeding these clouds with ice-nucleating particles (INPs), liquid droplets are converted to ice via heterogeneous freezing, triggering the Wegener-Bergeron-Findeisen (WBF) process that further depletes liquid water (Toll et al., 2024; Villanueva et al., 2025). The resulting glaciated cloud has a lower optical depth and shorter lifetime, reducing its longwave cloud radiative effect; over the polar oceans in winter, where mixed-phase clouds exert a net longwave warming that dominates over shortwave cooling, MCT thus produces a net surface cooling (Villanueva et al., 2022). Despite growing interest in MCT as a polar climate intervention, no coordinated multi-model protocol had previously been proposed; here we report initial findings from a first multi-model intercomparison effort – MCT-MIP Level 0 – and outline a CMIP7-aligned Level 1 protocol (MCT-L1).

#### 4.3.1 Level 0: Initial multi-model results

The Level 0 protocol was designed to be broadly implementable: atmosphere-only simulations with prescribed, fixed sea-surface temperatures and sea-ice fractions. Perturbations were done over the polar ocean domain (including sea-ice) poleward of  $60^{\circ}\text{N}$  and  $60^{\circ}\text{S}$ . This correspond to spatially uniform, winter-only (Nov, Dec, Jan, and Feb) additions to the dust cloud-borne concentration that is used as input for calculating droplet freezing, alongside an unperturbed control. The perturbation strength was  $10^4$ ,  $10^5$ , and  $10^6 \text{ L}^{-1}$ . Because only the inputs to the droplet-freezing calculations were perturbed, this can be interpreted as a “transparent” aerosol perturbation, decoupled from any side effects associated with direct radiative effects. Simulations used present-day (year 2000; repeating if possible) boundary conditions and ran for a minimum of 5 years (2 years for nudged models), with a 1-year spin-up discarded for free-running integrations. Four models participated (Table 6): ECHAM-HAM, ICON-HAM, CESM2, and E3SMv3.

The spatial distribution of the cloud radiative effect (CRE) response during the November–February season (NDJF) is shown in Figure 7 for all four models at the mid INP level ( $10^2 \text{ cm}^{-3}$ ). Three of the four models produce a net cooling with increasing INP concentration, consistent with the expected MCT mechanism; E3SMv3 is an outlier, showing a warming response.



	<b>ECHAM-HAM</b>	<b>ICON-HAM</b>
Resolution	T63 (~1.875°), 96×192	R2B4 (~160 km), 20,480 cells
Vertical levels	31	47
Grid type	Gaussian	Icosahedral
Microphysics	P3, N12	2-mom., N12 & L06
Run length	25 yr (MLO) & 2 yr (nudged)	5 yr (nudged)
	<b>CESM2</b>	<b>E3SM v3</b>
Resolution	0.9°, 192×288	Ne30 (~1°), 21,600 cols
Vertical levels	32	80
Grid type	Regular lat-lon	Cubed-sphere
Microphysics	2-mom., Wang et al. 2014	P3, Wang et al. 2014
Run length	5 yr	5 yr

**Table 6.** Models participating in MCT-MIP Level 0, with their atmospheric grid and run configuration. MLO: Mixed-Layer Ocean. N12: Niemand et al. (2012); L06: Lohmann and Diehl (2006).

The Arctic-mean (60–90°N) NDJF responses of CRE, ice water path (IWP), liquid water path (LWP), and total water path (TWP; from the Cloud\_cci v3 product, Stengel et al. 2020) as a function of INP concentration are shown in Figure 8. CESM2 and ICON-HAM show a clear reduction in LWP with increasing INP concentration, consistent with the MCT mechanism, while E3SMv3 maintains very low LWP across all perturbation levels. Note that the ECHAM-HAM (MLO) configuration is shown for reference only; this idealized perturbation (Villanueva et al., 2022) was designed to maximize the droplet freezing rate (1% of droplets freeze per hour) and is not directly comparable to the dust-based INP seeding protocol used by the other simulations.

Investigation of the E3SMv3 case reveals a base state in which cloud ice strongly dominates over liquid (Figure 8b–c), suggesting that clouds in the perturbed domain are already in a saturated-ice regime where the WBF process cannot operate effectively and additional INPs likely suppress the WBF process even further, by decreasing the size of ice particles and slowing down riming and sedimentation. This result underlines the importance of constraining the mixed-phase cloud liquid/ice partition against observations in future intercomparisons.

The sensitivity of the cooling to INP concentration also varies substantially across the three responding models, and the lowest perturbation level ( $10^4 \text{ L}^{-1}$ ) already produces a strong response in total water path (Figure 8c), motivating the extension to lower concentrations in the next Level 1 intercomparison.

### 4.3.2 Level 1 protocol: First MCT contribution to GeoMIP

As in Level 0, MCT-L1 simulations are atmosphere-only with prescribed present-day SSTs and sea-ice fractions, with the INP perturbation implemented as a transparent addition to background dust (modifying only freezing rates, without a new tracer). The perturbation range is revised to  $10^2$ ,  $10^4$ , and  $10^6 \text{ L}^{-1}$  to better characterize the onset of the MCT response at low concentrations. In addition, participating models are encouraged to run a complementary batch in which the background INP concentration from the control is multiplied by  $10^{-2}$ ,  $10^{-4}$ , and  $10^{-6}$ , probing the sensitivity to a lower INP mean-state



concentration. It is expected that such experiments can help clarify how the INP mean-state of models affects their MCT response.

Group	Simulation	INP perturbation	Type
Control	CTRL	none	—
MCT-L1-Background	INP_low_back	$\text{CTRL} \times 10^{-6} \text{ L}^{-1}$	multiplicative
	INP_mid_back	$\text{CTRL} \times 10^{-4} \text{ L}^{-1}$	multiplicative
	INP_high_back	$\text{CTRL} \times 10^{-2} \text{ L}^{-1}$	multiplicative
MCT-L1-Seeding	INP_low_seed	$\text{CTRL} + 10^2 \text{ L}^{-1}$	additive
	INP_mid_seed	$\text{CTRL} + 10^4 \text{ L}^{-1}$	additive
	INP_high_seed	$\text{CTRL} + 10^6 \text{ L}^{-1}$	additive

**Table 7.** MCT-L1 simulation matrix (7 simulations total). MCT-L1-Seeding perturbations add a spatially uniform INP concentration to the background dust; MCT-L1-Background perturbations scale the control background by the given factor.

565 The full set of 7 simulations (1 CTRL + 3 MCT-L1-Seeding + 3 MCT-L1-Background) is designed to map the complete range of mixed-phase cloud responses to INP forcing and to reveal base-state biases of the kind identified in Level 0.

### 4.3.3 Required output

Correctly attributing the MCT response requires cloud fields at higher temporal resolution than standard monthly means; in particular, monthly-mean bulk phase ratios are insufficient to reproduce satellite-based cloud-top phase climatologies stratified by temperature. In addition to the standard 2D monthly-mean fields from Level 0, the Level 1 protocol therefore requires:

- **Daily sampled instantaneous values** of 2D fields (TOA, ATM, and BOA clear-sky and all-sky radiative fluxes) and 3D temperature and cloud fields (cloud water content and particle number for liquid and ice; snow and rain if available);
- **COSP forward-simulator** output (CALIPSO/ISCCP diagnostics) for direct comparison with satellite cloud-top-phase retrievals;
- **Glaciation process rates** (daily sampled instantaneous values): at least heterogeneous droplet freezing rate, ice depositional growth rate (WBF), and ice/snow riming rate. Because daily 3D process rates are very expensive to store, we encourage the use of online 2D column-integrated, mixed-phase-integrated, and cloud-top alternatives, which will otherwise be calculated offline.

### 4.3.4 Nudging

580 Wind-only nudging to ERA5 reanalysis is strongly encouraged to suppress internal variability and enable meaningful multi-model comparison; free-running simulations with a minimum of 10 years are an acceptable alternative.



### ΔCRE spatial maps — NDJF

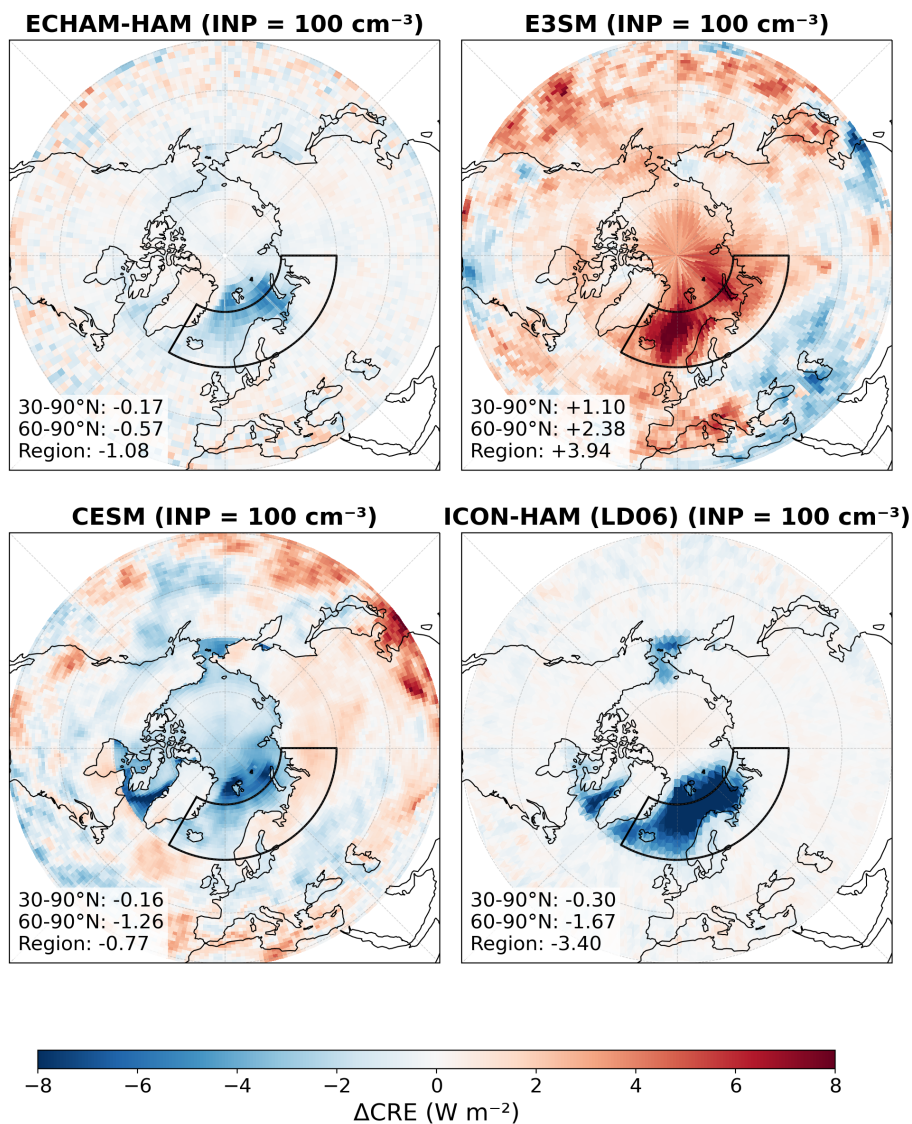


**Figure 7.** Spatial maps of the net cloud radiative effect perturbation ( $\Delta\text{CRE}$ ,  $\text{W m}^{-2}$ ) during NDJF for the mid INP level ( $10^2 \text{ cm}^{-3}$ ) relative to the control simulation, for all four MCT-MIP Level 0 models. Numbers inset in each panel give the area-weighted mean  $\Delta\text{CRE}$  over 30–90°N, 60–90°N, and the outlined target region (60–90°N, 30°W–90°E, i.e. the North Atlantic–European sector). Blue shading indicates cooling; red shading indicates warming. ECHAM-HAM, CESM2, and ICON-HAM all produce a net negative  $\Delta\text{CRE}$  poleward of 60°N, consistent with the MCT mechanism, while E3SMv3 shows a widespread warming response driven by a base state dominated by very low liquid water content.

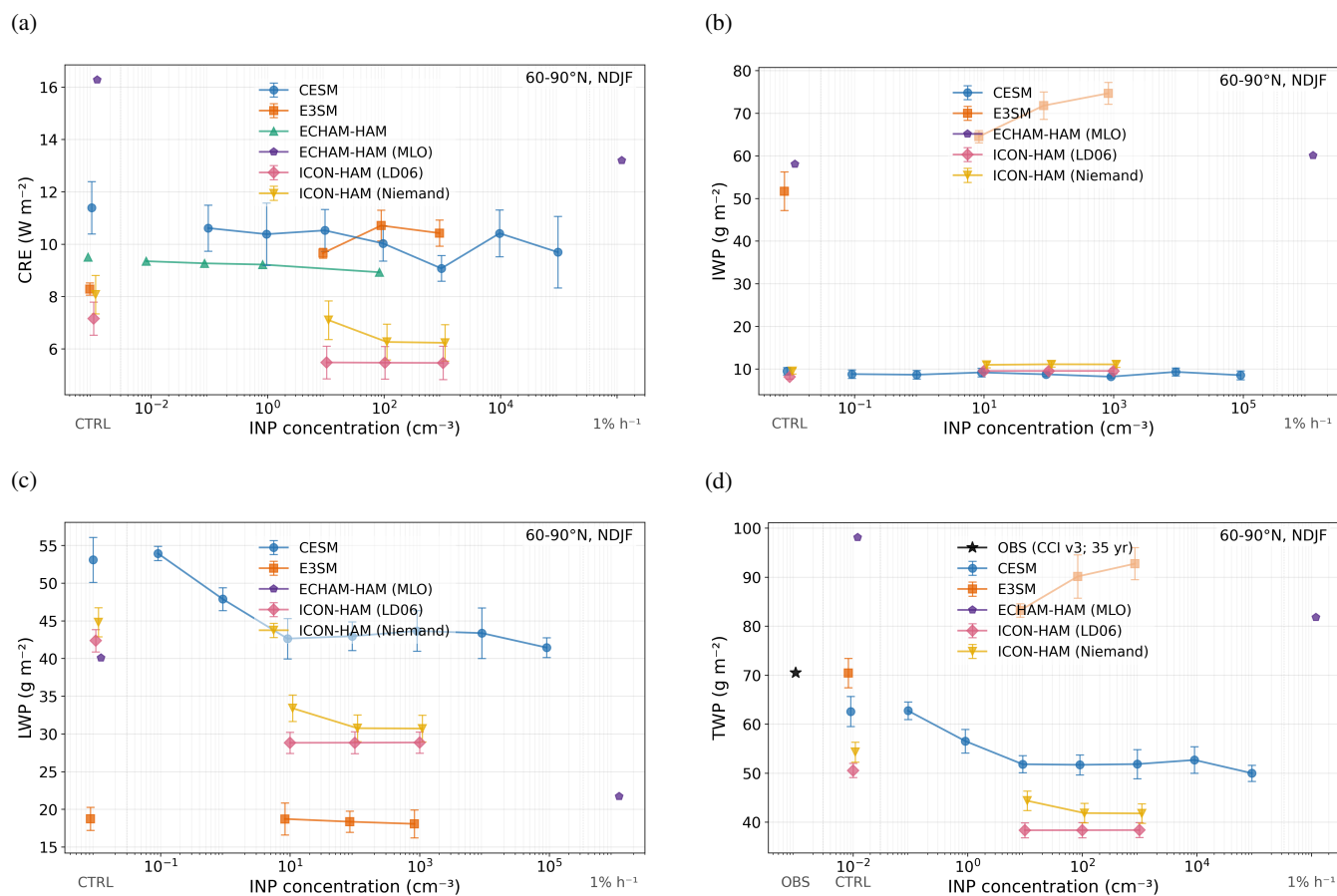


**Figure 8.** Arctic-mean (60–90°N) NDJF response as a function of INP concentration for all MCT-MIP Level 0 models and configurations. (a) Net cloud radiative effect (CRE, W m<sup>-2</sup>); the control value is shown at the left margin. (b) Ice water path (IWP, g m<sup>-2</sup>); E3SM’s anomalously high and monotonically increasing IWP explains its warming CRE response. (c) Liquid water path (LWP, g m<sup>-2</sup>). (d) Total water path (TWP, g m<sup>-2</sup>). Error bars denote the inter-annual standard error of the mean.



Experiment name	Description of intervention	Underlying emission scenario	Period
G2-SAI-1DOF	Equal yearly injections of SO <sub>2</sub> at 30°N and 30°S to maintain GMSAT at PI level	1%CO <sub>2</sub>	0-150
G2-SAI-3DOF	Yearly injections of SO <sub>2</sub> at different latitudes to maintain 3 temperature targets using feedback controller	1%CO <sub>2</sub>	0-150
SAI-SolidMIP-Timeslice	Yearly injection of 5 Tg mass of various solid materials at 30°N and 30°S	fixed climate (near-present)	0-30

**Table 8.** Process understanding Tier 2 experiments. GMSAT = Global Mean Surface Air Temperature; SAI = Stratospheric Aerosol Injection; DOF = Degrees of Freedom. As we do not expect all modeling teams to perform these experiments, and they are not comprehensive nor prescriptive, no total for the years of simulation is provided.

#### 4.4 Process understanding Tier 2 experiments

This set of experiments is more targeted towards “idealized” scenarios and, like the preparatory experiments, is more targeted towards better understanding of the outcomes of the Tier 1 and some Tier 2 experiments.

585

**G2 simulations** The G2 experiment was proposed by the original paper introducing GeoMIP (Kravitz et al., 2011). In the G2 experiment, solar dimming was used to offset forcing from annual 1% increases in CO<sub>2</sub> concentrations (“1%CO<sub>2</sub> forcing”) against a pre-industrial control (PIcontrol) background. Future warming scenarios include not only GHG forcing, but also evolving aerosol emissions and land use; modeling SRM against a PI control background allows for an evaluation of the impacts of SRM in the absence of these changes. Additionally, beginning SRM at the same time as GHG forcing begins means there is no long-term drift in the background climate state at the start of the experiment.

590

Lee et al. (2026a) revisited the G2 experiment by modeling contemporary SAI strategies against PI control + 1%CO<sub>2</sub> forcing for 150 years, with injection beginning the same year as 1%CO<sub>2</sub> forcing begins. They simulated two different strategies: the 1-DOF strategy used in G6-SAI (hemispherically symmetrical injection at 30° to manage global mean temperature) and the 3-DOF strategy used in ARISE-SAI-1.5 (independent injections at 30°N, 15°N, 15°S, and 30°S to manage global mean temperature and the interhemispheric and equator-to-pole temperature gradients simultaneously). Modeling groups interested in understanding the long-term impacts of SAI, and in the importance of background scenario on SAI impacts, should consider running similar experiments.

595

**SAI-SolidMIP-Timeslice simulations** In addition to the G7-1.5K-SAI-Solid experiment, there is another, time-slice, experiment with solid particles for SAI that is being developed by some in the community, currently consisting of two models (SOCOL-AERv2, (Vattioni et al., 2024b) and WACCM6-CARMA, (Tilmes et al., 2026)) with sectional aerosol treatment. While some activities are coordinated with GeoMIP Tier 1 experiments earlier described in this paper, the SAI-SolidMIP-Timeslice experiment follows its own protocol to focus on process understanding in an idealized setting. The

600



605 experiment design is similar to the  $\text{SO}_2/\text{H}_2\text{SO}_4$  protocols described in Weisenstein et al. (2021), based on the atmospheric state fixed to 2040 (this includes all standard forcing such as, GHG, ODS levels, tropospheric aerosols, etc.) and the ocean is prescribed with decadal (2020-2029) climatologies of SST and sea ice cover. This climatically stable setting is then used to test various materials under symmetrical  $30^\circ\text{N}$  and  $30^\circ\text{S}$  single-point constant injections of 5 Tg of material per year. Such a configuration allows intercomparing microphysical and transport processes of solid particles and testing their further upgrades such as new measurements of refractive indices and surface chemistry. Optical properties resulting from these experiments will be then provided to the rest of the SAI community to have a closer look at the uncertainties of the responses in stratospheric dynamics, stratospheric water vapor and stratosphere-troposphere coupling. Chemical effects will be omitted in this first step of involving a wider community, due to the large uncertainties and ongoing laboratory activities associated with chemical reactions on alternative materials.

## 5 Data request and opportunities

615 Modeling centers performing GeoMIP simulations should pay close attention to the various data request efforts spearheaded under CMIP7 (Juckes et al., 2025). In particular, the data request efforts for the Atmosphere (Dingley et al., 2025), Earth System (McPartland et al., 2025) and Ocean and Sea Ice (Fox-Kemper et al., 2025) could be particularly important. Furthermore, opportunities to include variables needed by the Inter-Sectoral Impact Model Intercomparison Project (ISIMIP3a) (Frieler et al., 2024) should also be considered.

620

Simulation of MCB depends on a series of aerosol and cloud processes that must be parameterized in ESMs. Understanding how different processes contribute to inter-model variation in MCB forcing is crucial for constraining the potential cooling from MCB and developing models that can more credibly represent MCB interventions. Variables from the "Diagnosing Radiative Forcing" and "Understanding the role of atmospheric composition for air quality and climate change" opportunities from Dingley et al. (2025) highlight key variables relevant for diagnosing MCB aerosol and cloud responses. Additionally, cloud condensation nuclei concentrations and subgrid vertical velocity used in prognostic aerosol activation schemes can enable clearer comparisons of cloud droplet activation rates across models, especially for Inj-seasalt-midlat-SST.

High-frequency surface output could be considered in order to investigate the potential for SRM to interact with energy systems (Kumler et al., 2025), as done in Baur et al. (2024b, a): this would require 3 or 6 hourly surface winds and incoming solar radiation, as well as temperature and other meteorological variables such as sea level pressure and humidity that could also be used to diagnose cyclonic activity under SRM (Gabriel Martins Ribeiro et al., 2025). Acknowledging the high burden of providing such data (on both the storage and the analyses side), modeling centers could provide it only for specific time slices (such as the first 10 and last 10 years of simulations for a specific cases). In terms of radiation fluxes, we strongly recommend the inclusion of downwelling diffuse shortwave radiation (rsdsdiff). Although sometimes omitted in standard data requests, this variable is essential to accurately assess both crop photosynthesis efficiency and solar power generation under aerosol-altered

630  
635



atmospheric conditions. Providing these variables will greatly enhance the ability of the cross-sectoral impacts community to evaluate the consequences arising from the GeoMIP7 experiments.

Another area with growing interests within the SRM research community that could also leverage high-frequency output is related to analyze extreme events (Tye et al., 2022); this can be better done by using ESM data as boundary conditions  
640 for downscaling efforts using Regional Climate Models (RCM) to get better regional information (Wang et al., 2022; Sun et al., 2026), or using ESM output as a driver for impacts models (Wang et al., 2022). In the case of dynamical downscaling, the models require vertically resolved, sub-daily information, which can be burdensome to save, standardize, and transfer. Nevertheless, the community is clearly at a point where it is ready to engage with these issues, necessitating an explicit request for daily and sub-daily data. To hopefully ease the burden on modeling and analysis groups, we have created a prioritized list  
645 of variables that we would like models to save with these temporal frequencies, if they are interested in having their models contributing to dynamical downscaling efforts. A list of the high-frequency output that is needed for these kind of assessments is presented in Table 9.

Lastly, while much of the climate modeling focus has been directed toward surface and tropospheric impacts, critical gaps remain in understanding the effects of SRM on the stratosphere itself (Tilmes et al., 2022; Bednarz et al., 2022). Future analyses  
650 within GeoMIP7 should continue addressing how stratospheric aerosols may alter large-scale atmospheric architecture, including regarding changes in stratospheric circulation, tropopause height and the modulation of stratospheric contraction (Pisoft et al., 2021). Addressing many of these structural changes requires robust stratospheric representation; thus, we encourage the community to rely on high-top models capable of capturing such changes for SAI simulations.



Variable Name	Temporal Frequency	Vertically Resolved?	Purpose
Horizontal Wind (ua, va)	6-hourly	Yes	Boundary conditions for regional models
Surface Wind Speed (sfcWind)	6-hourly	N/A	Boundary conditions for regional models
Temperature (ta)	6-hourly	Yes	Boundary conditions for regional models
Surface (skin) Temperature (ts)	6-hourly	N/A	Boundary conditions for regional models
2m temperature (tas)	daily	N/A	Extreme events analysis
Daily maximum near-surface temperature (tasmax)	daily	N/A	Extreme events analysis
Daily minimum near-surface temperature (tasmin)	daily	N/A	Extreme events analysis
Relative humidity (hur)	6-hourly	Yes	Boundary conditions for regional models
Sea level pressure (psl)	6-hourly	N/A	Boundary conditions for regional models
Surface pressure (ps)	6-hourly	N/A	Boundary conditions for regional models
Soil liquid water	daily	N/A	Boundary conditions for regional models
Snow fraction	daily	N/A	Boundary conditions for regional models
Soil temperature (tsl)	daily	N/A	Boundary conditions for regional models
Water or lake temperature	daily	N/A	Boundary conditions for regional models
Surface radiative fluxes (rsds, rsus, rlds, rlus, rldscs, rldscs)	daily	N/A	Impacts modeling

**Table 9.** List of high-frequency output that would be required to drive RCMs under SAI scenarios. Between brackets is the CMIP standard variable name ID, when available.



## 655 6 Conclusions

Earth system modeling of different SRM techniques has substantially grown our collective understanding of their potential to avert some consequences of anthropogenic global warming, as well as potential unintended consequences on other climate variables. With this, we do not claim that all questions have been answered; rather, an increased exploration of the size of the potential space of these intervention has shown that deep care should be taken in claiming that, generically, “SRM would do X  
660 to system Y”. Recent research has shown that how the specific SRM techniques is simulated, in terms of location, timeliness, underlying scenario, and magnitude of intervention, all matter when discussing the potential impacts, and while some broad consequences are independent of these details, many are not. Similarly, a renewed interest in the physical and ecological impacts, also driven by an expansion of the community of users for such simulations, has led to a deeper understanding of the sources of uncertainty in such simulations.

665

The GeoMIP community has found that the need to increase the exploration of the scenario space, the need to be able to pinpoint specific physical uncertainties and sources of inter-model spread, and the need to maintain a simple system that is usable and understandable by a broad set of users are all very relevant needs that must be balanced, and no perfect answer exists. The framework GeoMIP is proposing for CMIP7 tries to address many of these challenges, and has matured over many  
670 annual workshops with intense discussions. We have aimed to keep proposed experiments simple, yet plausible, to enable the community to both understand more easily sources of uncertainties while relying on a similar scenario framework as other MIPs. We have accompanied the main experiments with more simple experiments that are both useful for diagnosing responses and that can be potentially leveraged to build emulators that can accompany the main simulations to expand the scenario space beyond what is computationally feasible in ESMs. And, this time, we have also proposed a more flexible framework in which  
675 modeling teams can maintain a common basis and yet explore specific scenarios that are of interest to them.

Simplicity is a deliberate choice, rather than the product of naivete. The main goal of GeoMIP remains that of highlighting sources of agreement and disagreement across different models, and that is undoubtedly easier to do in somewhat simplified modeling scenarios. This should not be taken (and indeed, the GeoMIP community has never done so) as a claim that the scenarios we produce are aiming to be prescriptive or predictive. A clearer understanding and disentangling of physical impacts  
680 has the potential to clarify the implications of what could be “real-world” deployments, which can serve as an input for other fields of research, as well as interdisciplinary research, to expand the space of assessment and understanding of risks beyond climate science (Tilmes et al., 2024; Beckage et al., 2025; Estrada et al., 2026).

685 *Code and data availability.* The near-surface air temperature and SAI injection magnitude data needed to reproduce Figures 2 and 4 is also available on Zenodo <https://doi.org/10.5281/zenodo.19556593> (Duffey, 2026). The ARISE-SAI simulations used in Figure 2 are publicly available via the NCAR Geoscience Data Exchange <https://gdex.ucar.edu/datasets/d651059/> (Richter, 2025). Figure 3 is taken from Lee



et al. (2026b) and the data to reproduce it is available on Zenodo <https://doi.org/10.5281/zenodo.17613419> (Lee et al., 2025b). Code to reproduce Figures 2 and 4 for the G6-1.5K-HiLLA simulations is also available on Zenodo <https://doi.org/10.5281/zenodo.19582298> (Duffey and Wang, 2026), or on Github at [https://github.com/alistairduffey/GeoMIP\\_for\\_CMIP7\\_analysis\\_code](https://github.com/alistairduffey/GeoMIP_for_CMIP7_analysis_code). The G6-1.5K-MCB data required for Figure 5, along with the analysis code to reproduce it, is available on Zenodo <https://doi.org/10.5281/zenodo.19582532> (Hirasawa et al., 2025b). Data for the level 0 MCT MIP is available on Zenodo <https://doi.org/10.5281/zenodo.19665403> (Villanueva et al., 2026). Further monthly data for the G6-1.5K-SAI and G6-1.5K-MCB simulations is available in the respective publications cited in this manuscript; <https://doi.org/10.5281/zenodo.17613418> (Lee et al., 2026b) and <https://doi.org/10.5281/zenodo.17525291> (Hirasawa et al., 2025a).

695 *Author contributions.* DV conceptualized the study. DV, AD, MH, HH and WL prepared the original draft. AD, MH, HH, WL and CW performed the formal analyses. All authors revised the manuscript and provided meaningful suggestions throughout the process.

*Competing interests.* At least one of the co-authors is a member of the editorial board of GMD.

*Acknowledgements.* DV would like to acknowledge the Quadrature Climate Foundation for their support in providing travel grants to the GeoMIP annual meetings, as well as the GeoMIP community for their continued engagement and contribution. Support for BK was provided in part by NOAA's Climate Program Office, Earth's Radiation Budget (ERB) (Grant NA22OAR4310479), and the Indiana University Environmental Resilience Institute. Support for EMB has been provided by the National Oceanic and Atmospheric Administration (NOAA) cooperative agreement (NA22OAR4320151), the Earth's Radiative Budget (ERB) program, and Reflective's Fellowship program. MS and SW were supported by JSPS KAKENHI Grant Number JP25K03324. MIROC-ES2H simulations were supported by the MEXT Program for Advanced Studies of Climate Change Projection (SENTAN) Grant Number JPMXD0722681344 and performed using the Earth Simulator at JAMSTEC. AR was supported by NSF grant AGS-2017113.

700  
705



## References

- Ahlm, L., Jones, A., Stjern, C. W., Muri, H., Kravitz, B., and Kristjánsson, J. E.: Marine cloud brightening – as effective without clouds, *Atmospheric Chemistry and Physics*, 17, 13 071–13 087, <https://doi.org/10.5194/acp-17-13071-2017>, 2017.
- Alterskjaer, K. and Kristjánsson, J.: The sign of the radiative forcing from marine cloud brightening depends on both particle size and injection amount, *Geophysical Research Letters*, 40, 210–215, 2013.
- Alterskjaer, K., Kristjánsson, J. E., Boucher, O., Muri, H., Niemeier, U., Schmidt, H., Schulz, M., and Timmreck, C.: Sea-salt injections into the low-latitude marine boundary layer: The transient response in three Earth system models, *Journal of Geophysical Research: Atmospheres*, 118, 12,195–12,206, <https://doi.org/https://doi.org/10.1002/2013JD020432>, 2013.
- Baur, S., Nauels, A., Nicholls, Z., Sanderson, B. M., and Schleussner, C.-F.: The deployment length of solar radiation modification: an interplay of mitigation, net-negative emissions and climate uncertainty, *Earth System Dynamics*, 14, 367–381, <https://doi.org/10.5194/esd-14-367-2023>, 2023.
- Baur, S., Sanderson, B. M., Séférian, R., and Terray, L.: Solar radiation modification challenges decarbonization with renewable solar energy, *Earth System Dynamics*, 15, 307–322, <https://doi.org/10.5194/esd-15-307-2024>, 2024a.
- Baur, S., Sanderson, B. M., Séférian, R., and Terray, L.: Change in Wind Renewable Energy Potential Under Stratospheric Aerosol Injections, *Earth's Future*, 12, e2024EF004 575, <https://doi.org/https://doi.org/10.1029/2024EF004575>, e2024EF004575 2024EF004575, 2024b.
- Baur, S., Sanderson, B. M., Séférian, R., and Terray, L.: Change in negative emission burden between an overshoot versus peak-shaved stratospheric aerosol injection pathway, *Earth System Dynamics*, 16, 667–681, <https://doi.org/10.5194/esd-16-667-2025>, 2025.
- Beckage, B., Lacasse, K., Raimi, K. T., and Vioni, D.: Models and scenarios for solar radiation modification need to include human perceptions of risk, *Environmental Research: Climate*, 4, 023 003, <https://doi.org/10.1088/2752-5295/add42>, 2025.
- Bednarz, E. M., Vioni, D., Banerjee, A., Braesicke, P., Kravitz, B., and MacMartin, D. G.: The Overlooked Role of the Stratosphere Under a Solar Constant Reduction, *Geophysical Research Letters*, 49, e2022GL098 773, <https://doi.org/https://doi.org/10.1029/2022GL098773>, e2022GL098773 2022GL098773, 2022.
- Bednarz, E. M., Vioni, D., Kravitz, B., Jones, A., Haywood, J. M., Richter, J., MacMartin, D. G., and Braesicke, P.: Climate response to off-equatorial stratospheric sulfur injections in three Earth system models – Part 2: Stratospheric and free-tropospheric response, *Atmospheric Chemistry and Physics*, 23, 687–709, <https://doi.org/10.5194/acp-23-687-2023>, 2023.
- Bednarz, E. M., Goddard, P. B., MacMartin, D. G., Vioni, D., Bailey, D., and Danabasoglu, G.: Stratospheric Aerosol Injection Could Prevent Future Atlantic Meridional Overturning Circulation Decline, But Injection Location is Key, *Earth's Future*, 13, e2025EF005 919, <https://doi.org/https://doi.org/10.1029/2025EF005919>, e2025EF005919 2025EF005919, 2025a.
- Bednarz, E. M., Haywood, J. M., Vioni, D., Butler, A. H., and Jones, A.: How marine cloud brightening could also affect stratospheric ozone, *Science Advances*, 11, eadu4038, <https://doi.org/10.1126/sciadv.adu4038>, 2025b.
- Brody, E., Vioni, D., Bednarz, E. M., Kravitz, B., MacMartin, D. G., Richter, J. H., and Tye, M. R.: Kicking the can down the road: understanding the effects of delaying the deployment of stratospheric aerosol injection, *Environmental Research: Climate*, 3, 035 011, 2024.
- Burgess, M. G., Ritchie, J., Shapland, J., and Pielke, R.: IPCC baseline scenarios have over-projected CO<sub>2</sub> emissions and economic growth, *Environmental Research Letters*, 16, 014 016, 2020.
- Cao, L., Duan, L., Bala, G., and Caldeira, K.: Simultaneous stabilization of global temperature and precipitation through cocktail geoengineering, *Geophysical Research Letters*, 44, 7429–7437, <https://doi.org/https://doi.org/10.1002/2017GL074281>, 2017.



- Chen, C.-C., Richter, J., Lee, W. R., Tye, M., MacMartin, D. G., and Kravitz, B.: Climate impact of marine cloud brightening solar climate intervention under a susceptibility-based strategy simulated by CESM2, *Journal of Geophysical Research: Atmospheres*, 130, e2024JD041 245, 2025.
- 745 Clark, B., Xia, L., Robock, A., Tilmes, S., Richter, J. H., Vioni, D., and Rabin, S. S.: Optimal climate intervention scenarios for crop production vary by nation, *Nature Food*, 4, 902–911, <https://doi.org/10.1038/s43016-023-00853-3>, 2023.
- Clark, S., King, A. D., Brown, J. R., Cassidy, L. J., de Asenjo, E. A., and Ziehn, T.: The reversibility of local and regional temperature extremes in CDRMIP, *ESS Open Archive*, 2025, <https://doi.org/10.22541/essoar.176556040.07127388/v1>, 2025.
- 750 Dingley, A., Anstey, J. A., Abalos, M., Abraham, C., Bergman, T., Bock, L., Fiddes, S., Hassler, B., Kramer, R. J., Luo, F., O'Connor, F. M., Šácha, P., Simpson, I. R., Wilcox, L. J., and Zelinka, M. D.: CMIP7 Data Request: Atmosphere Priorities and Opportunities, *EGUsphere*, 2025, 1–54, <https://doi.org/10.5194/egusphere-2025-3189>, 2025.
- Duffey, A.: Temperature and injection magnitudes in G6-1.5K-SAI, G6-1.5K-HiLLA and SSP2-4.5, <https://doi.org/10.5281/zenodo.19556593>, 2026.
- 755 Duffey, A. and Wang, C.: *alistairduffey/GeoMIP\_for\_CMIP7\_analysis\_code: v0.0*, <https://doi.org/10.5281/zenodo.19582298>, 2026.
- Duffey, A., Henry, M., Smith, W., Tsamados, M., and Irvine, P. J.: Low-Altitude High-Latitude Stratospheric Aerosol Injection Is Feasible With Existing Aircraft, *Earth's Future*, 13, e2024EF005 567, <https://doi.org/10.1029/2024EF005567>, publisher: John Wiley & Sons, Ltd, 2025.
- Duffey, A., Lee, W., Wheeler, L., Irvine, P., Wagman, B., Henry, M., Vioni, D., Tsamados, M., and MacMartin, D.: The global climate response to High-Latitude Low-Altitude Stratospheric Aerosol Injection (HiLLA-SAI), *Earth System Dynamics*, 17, 353–385, 2026.
- 760 Dykema, J. A., Keith, D. W., and Keutsch, F. N.: Improved aerosol radiative properties as a foundation for solar geoengineering risk assessment, *Geophysical Research Letters*, 43, 7758–7766, <https://doi.org/10.1002/2016GL069258>, 2016.
- Eastham, S. D., Butler, A. H., Doherty, S. J., Gasparini, B., Tilmes, S., Bednarz, E. M., Burkhardt, U., Chiodo, G., Cziczko, D. J., Diamond, M. S., Keith, D. W., Leisner, T., MacMartin, D. G., Quaas, J., Rasch, P. J., Sourdeval, O., Steinke, I., Thompson, C., Vioni, D., Wood, R., Xia, L., and Yu, P.: Key Gaps in Models' Physical Representation of Climate Intervention and Its Impacts, *Journal of Advances in Modeling Earth Systems*, 17, e2024MS004 872, <https://doi.org/https://doi.org/10.1029/2024MS004872>, e2024MS004872 2024MS004872, 2025.
- 765 Egbebiyi, T. S., Ajayi, V. O., Arowolo, A. V., Ogunniyi, J., and Ogunjo, S.: The effect of solar radiation modification on agroclimatic indices in Africa, *Environmental Research: Climate*, 4, 035 003, <https://doi.org/10.1088/2752-5295/ade619>, 2025.
- Emme, E., Chen, C.-C., and Horowitz, H. M.: Impact of seasonality on climate outcomes for mid latitude marine cloud brightening, *Geophysical Research Letters*, 52, e2025GL115 359, 2025.
- 770 Estrada, F., Bastien-Olvera, B. A., Calderon-Bustamante, O., Altamirano, M. A., Muñoz-Sánchez, R., Moreno-Cruz, J., and Botzen, W.: Economic assessment of SRM under socio-political and geophysical tipping dynamics, *Environmental Research: Climate*, 5, 015 015, <https://doi.org/10.1088/2752-5295/ae33df>, 2026.
- Farley, J., MacMartin, D. G., Vioni, D., and Kravitz, B.: Emulating inconsistencies in stratospheric aerosol injection, *Environmental Research: Climate*, 3, 035 012, <https://doi.org/10.1088/2752-5295/ad519c>, 2024.
- 775 Farley, J., MacMartin, D. G., Vioni, D., Kravitz, B., Bednarz, E. M., Duffey, A., Henry, M., and Akherati, A.: A Climate Intervention Dynamical Emulator (CIDER) for scenario space exploration, *Geoscientific Model Development*, 19, 1809–1831, <https://doi.org/10.5194/gmd-19-1809-2026>, 2026.



- Feng, Z., Tan, M. L., Mahamud, M. A., Chuah, J., and Zhang, F.: Impacts of solar radiation modification on temperature extremes and heatwaves in Southeast Asia, *Weather and Climate Extremes*, 49, 100 789, <https://doi.org/https://doi.org/10.1016/j.wace.2025.100789>, 2025.
- Fox-Kemper, B., DeRepentigny, P., Treguier, A. M., Stepanek, C., O'Rourke, E., Mackallah, C., Meucci, A., Aksenov, Y., Durack, P. J., Feldl, N., Hernaman, V., Heuzé, C., Iovino, D., Madan, G., Marquez, A. L., Massonnet, F., Mecking, J., Samanta, D., Taylor, P. C., Tseng, W.-L., and Vancoppenolle, M.: CMIP7 Data Request: Ocean and Sea Ice Priorities and Opportunities, *EGUsphere*, 2025, 1–58, <https://doi.org/10.5194/egusphere-2025-3083>, 2025.
- Frieler, K., Volkholz, J., Lange, S., Schewe, J., Mengel, M., del Rocío Rivas López, M., Otto, C., Reyer, C. P. O., Karger, D. N., Malle, J. T., Treu, S., Menz, C., Blanchard, J. L., Harrison, C. S., Petrik, C. M., Eddy, T. D., Ortega-Cisneros, K., Novaglio, C., Rousseau, Y., Watson, R. A., Stock, C., Liu, X., Heneghan, R., Tittensor, D., Maury, O., Büchner, M., Vogt, T., Wang, T., Sun, F., Sauer, I. J., Koch, J., Vanderkelen, I., Jägermeyr, J., Müller, C., Rabin, S., Klar, J., Vega del Valle, I. D., Lasslop, G., Chadburn, S., Burke, E., Gallego-Sala, A., Smith, N., Chang, J., Hantson, S., Burton, C., Gädeke, A., Li, F., Gosling, S. N., Müller Schmied, H., Hattermann, F., Wang, J., Yao, F., Hickler, T., Marcé, R., Pierson, D., Thiery, W., Mercado-Bettín, D., Ladwig, R., Ayala-Zamora, A. I., Forrest, M., and Bechtold, M.: Scenario setup and forcing data for impact model evaluation and impact attribution within the third round of the Inter-Sectoral Impact Model Intercomparison Project (ISIMIP3a), *Geoscientific Model Development*, 17, 1–51, <https://doi.org/10.5194/gmd-17-1-2024>, 2024.
- Fuglesang, C. and de Herreros Miciano, M. G.: Realistic sunshade system at L1 for global temperature control, *Acta Astronautica*, 186, 269–279, <https://doi.org/https://doi.org/10.1016/j.actaastro.2021.04.035>, 2021.
- Gabriel Martins Ribeiro, J., Reboita, M. S., Machado Crespo, N., and Moore, J.: Impacts of stratospheric aerosol injection on precipitation and winds associated with extratropical cyclones in the Southern Hemisphere, *Environmental Research: Climate*, 4, 045 021, <https://doi.org/10.1088/2752-5295/ae228b>, 2025.
- Haywood, J. M., Jones, A., Bellouin, N., and Stephenson, D.: Asymmetric forcing from stratospheric aerosols impacts Sahelian rainfall, *Nature Climate Change*, 3, 660–665, <https://doi.org/10.1038/nclimate1857>, 2013.
- Haywood, J. M., Jones, A., Jones, A. C., Halloran, P., and Rasch, P. J.: Climate intervention using marine cloud brightening (MCB) compared with stratospheric aerosol injection (SAI) in the UKESM1 climate model, *Atmospheric Chemistry and Physics*, 23, 15 305–15 324, 2023.
- Haywood, J. M., Boucher, O., Lennard, C., Storelvmo, T., Tilmes, S., and Visionsi, D.: World Climate Research Programme light-house activity: an assessment of major research gaps in solar radiation modification research, *Frontiers in Climate*, Volume 7 - 2025, <https://doi.org/10.3389/fclim.2025.1507479>, 2025.
- Henry, M., Haywood, J., Jones, A., Dalvi, M., Wells, A., Visionsi, D., Bednarz, E. M., MacMartin, D. G., Lee, W., and Tye, M. R.: Comparison of UKESM1 and CESM2 simulations using the same multi-target stratospheric aerosol injection strategy, *Atmospheric Chemistry and Physics*, 23, 13 369–13 385, 2023.
- Henry, M., Hirasawa, H., Haywood, J., and Rasch, P. J.: Marine cloud brightening to cool the Arctic: An Earth system model comparison, *Earth's Future*, 13, e2025EF006 508, 2025.
- Hirasawa, H., Hingmire, D., Singh, H., Rasch, P. J., and Mitra, P.: Effect of regional marine cloud brightening interventions on climate tipping elements, *Geophysical Research Letters*, 50, e2023GL104 314, 2023.
- Hirasawa, H., Henry, M., Rasch, P. J., Wood, R., Doherty, S. J., Haywood, J., Wong, A., Lamarque, J.-F., Brody, E., and Wang, H.: G6-1.5 K-MCB: Marine Cloud Brightening Scenario design for the Geoengineering Model Intercomparison Project (GeoMIP) in CESM2. 1, E3SMv2. 0, and UKESM1. 1, *EGUsphere*, 2025, 1–35, 2025a.



- Hirasawa, H., Matthew, H., Wood, R., Doherty, S., Rasch, P., and Watanabe, S.: Data for "G6-1.5K-MCB: Marine Cloud Brightening Scenario design for the Geoengineering Model Intercomparison Project (GeoMIP)", <https://doi.org/10.5281/zenodo.17525291>, 2025b.
- Hirasawa, H., Henry, M., Mason, A. M., Rasch, P. J., Doherty, S. J., Wood, R., Haywood, J., and von Salzen, K.: Forcing Susceptibility and Climate Sensitivity to Midlatitude Marine Cloud Brightening, *Journal of Climate*, 39, 769–784, 2026.
- 820 Irvine, P., Emanuel, K., He, J., Horowitz, L. W., Vecchi, G., and Keith, D.: Halving warming with idealized solar geoengineering moderates key climate hazards, *Nature Climate Change*, 9, 295–299, <https://doi.org/10.1038/s41558-019-0398-8>, 2019.
- Jones, A., Haywood, J., and Boucher, O.: Climate impacts of geoengineering marine stratocumulus clouds, *Journal of Geophysical Research: Atmospheres*, 114, 2009.
- Jones, A., Haywood, J. M., Alterskjær, K., Boucher, O., Cole, J. N. S., Curry, C. L., Irvine, P. J., Ji, D., Kravitz, B., Egill Kristjánsson, J.,  
825 Moore, J. C., Niemeier, U., Robock, A., Schmidt, H., Singh, B., Tilmes, S., Watanabe, S., and Yoon, J.-H.: The impact of abrupt suspension of solar radiation management (termination effect) in experiment G2 of the Geoengineering Model Intercomparison Project (GeoMIP), *Journal of Geophysical Research: Atmospheres*, 118, 9743–9752, <https://doi.org/https://doi.org/10.1002/jgrd.50762>, 2013.
- Jörmann, A., Sukhodolov, T., Luo, B., Chiodo, G., Mann, G., and Peter, T.: REtrieval Method for optical and physical Aerosol Properties in the stratosphere (REMAPv1), *Geoscientific Model Development*, 18, 6023–6041, <https://doi.org/10.5194/gmd-18-6023-2025>, 2025.
- 830 Jukes, M., Taylor, K. E., Antonio, F., Brayshaw, D., Buontempo, C., Cao, J., Durack, P. J., Kawamiya, M., Kim, H., Lovato, T., Mackallah, C., Mizielinski, M., Nuzzo, A., Stockhause, M., Visoni, D., Walton, J., Turner, B., O'Rourke, E., and Dingley, B.: Baseline Climate Variables for Earth System Modelling, *Geoscientific Model Development*, 18, 2639–2663, <https://doi.org/10.5194/gmd-18-2639-2025>, 2025.
- Kim, H., Kim, H., Visoni, D., and Bednarz, E. M.: Sensitivity of Arctic sea ice recovery to stratospheric aerosol injection latitude, *npj Climate and Atmospheric Science*, 9, 24, 2025.
- 835 Kravitz, B., Robock, A., Boucher, O., Schmidt, H., Taylor, K. E., Stenchikov, G., and Schulz, M.: The Geoengineering Model Intercomparison Project (GeoMIP), *Atmospheric Science Letters*, 12, 162–167, <https://doi.org/10.1002/asl.316>, 2011.
- Kravitz, B., Forster, P. M., Jones, A., Robock, A., Alterskjær, K., Boucher, O., Jenkins, A. K., Korhonen, H., Kristjánsson, J. E., Muri, H., et al.: Sea spray geoengineering experiments in the geoengineering model intercomparison project (GeoMIP): Experimental design and  
840 preliminary results, *Journal of Geophysical Research: Atmospheres*, 118, 11–175, 2013.
- Kravitz, B., Robock, A., Tilmes, S., Boucher, O., English, J. M., Irvine, P. J., Jones, A., Lawrence, M. G., MacCracken, M., Muri, H., Moore, J. C., Niemeier, U., Phipps, S. J., Sillmann, J., Storelvmo, T., Wang, H., and Watanabe, S.: The Geoengineering Model Intercomparison Project Phase 6 (GeoMIP6): simulation design and preliminary results, *Geoscientific Model Development*, 8, 3379–3392, <https://doi.org/10.5194/gmd-8-3379-2015>, 2015.
- 845 Kravitz, B., MacMartin, D. G., Wang, H., and Rasch, P. J.: Geoengineering as a design problem, *Earth System Dynamics*, 7, 469–497, <https://doi.org/10.5194/esd-7-469-2016>, 2016.
- Kravitz, B., Lamarque, J.-F., Tribbia, J. J., Tilmes, S., Vitt, F., Richter, J. H., MacMartin, D. G., and Mills, M. J.: First Simulations of Designing Stratospheric Sulfate Aerosol Geoengineering to Meet Multiple Simultaneous Climate Objectives, *Journal of Geophysical Research: Atmospheres*, 122, 12,616–12,634, <https://doi.org/10.1002/2017jd026874>, 2017.
- 850 Kumar, J., Jung, G.-Y., Kapoor, T. S., Mishra, R., and Chakrabarty, R. K.: Strong light absorption by sp hybridized carbon impurities in diamond dust, *Journal of Aerosol Science*, 194, 106 767, <https://doi.org/10.1016/j.jaerosci.2026.106767>, 2026.



- Kumler, A., Kravitz, B., Draxl, C., Vimmerstedt, L., Benton, B., Lundquist, J. K., Martin, M., Buck, H. J., Wang, H., Lennard, C., and Tao, L.: Potential effects of climate change and solar radiation modification on renewable energy resources, *Renewable and Sustainable Energy Reviews*, 207, 114934, <https://doi.org/https://doi.org/10.1016/j.rser.2024.114934>, 2025.
- 855 Laakso, A., Snyder, P. K., Liess, S., Partanen, A.-I., and Millet, D. B.: Differing precipitation response between solar radiation management and carbon dioxide removal due to fast and slow components, *Earth System Dynamics*, 11, 415–434, <https://doi.org/10.5194/esd-11-415-2020>, 2020.
- Lee, W., MacMartin, D., Vioni, D., and Kravitz, B.: Expanding the design space of stratospheric aerosol geoengineering to include precipitation-based objectives and explore trade-offs, *Earth System Dynamics*, 11, 1051–1072, <https://doi.org/10.5194/esd-11-1051-2020>,  
860 2020.
- Lee, W. R., MacMartin, D. G., Vioni, D., Kravitz, B., Chen, Y., Moore, J. C., Leguy, G., Lawrence, D. M., and Bailey, D. A.: High-Latitude Stratospheric Aerosol Injection to Preserve the Arctic, *Earth's Future*, 11, e2022EF003052, <https://doi.org/https://doi.org/10.1029/2022EF003052>, e2022EF003052 2022EF003052, 2023.
- Lee, W. R., Chen, C.-C., Richter, J., MacMartin, D. G., and Kravitz, B.: First simulations of feedback algorithm-regulated marine cloud  
865 brightening, *Geophysical Research Letters*, 52, e2024GL113728, 2025a.
- Lee, W. R., Vioni, D., Wagman, B. M., Wentland, C. R., Kravitz, B., Watanabe, S., Sekiya, T., Jones, A., Haywood, J., Henry, M., and Bednarz, E. M.: Data for "G6-1.5K-SAI and G6sulfur: changes in impacts and uncertainty depending on stratospheric aerosol injection strategy in the Geoengineering Model Intercomparison Project", <https://doi.org/10.5281/zenodo.17613419>, 2025b.
- Lee, W. R., Tilmes, S., and Bednarz, E. M.: Exploring divergent long-term stratospheric aerosol injection scenarios with the G2-SAI and  
870 ARISE-hybrid experiments, *EGUsphere*, 2026, 1–23, <https://doi.org/10.5194/egusphere-2026-1004>, 2026a.
- Lee, W. R., Vioni, D., Wagman, B. M., Wentland, C. R., Kravitz, B., Watanabe, S., Sekiya, T., Jones, A., Haywood, J., Henry, M., and Bednarz, E. M.: G6-1.5K-SAI and G6sulfur: changes in impacts and uncertainty depending on stratospheric aerosol injection strategy in the Geoengineering Model Intercomparison Project, *EGUsphere*, 2025, 1–33, <https://doi.org/10.5194/egusphere-2025-5742>, 2026b.
- Lenton, T. M., Milkoreit, M., Willcock, S., Abrams, J. F., Armstrong McKay, D. I., Buxton, J. E., Donges, J. F., Loriani, S., Wunderling,  
875 N., Alkemade, F., Barrett, M., Constantino, S., Powell, T., Smith, S. R., Boulton, C. A., Pinho, P., Dijkstra, H. A., Pearce-Kelly, P., Roman-Cuesta, R. M., and Dennis, D.: The Global Tipping Points Report 2025, Tech. rep., University of Exeter, Exeter, UK, 2025.
- Li, Q., Meidan, D., Hess, P., Añel, J. A., Cuevas, C. A., Doney, S., Fernandez, R. P., van Herpen, M., Höglund-Isaksson, L., Johnson, M. S., Kinnison, D. E., Lamarque, J.-F., Röckmann, T., Mahowald, N. M., and Saiz-Lopez, A.: Global environmental implications of atmospheric methane removal through chlorine-mediated chemistry-climate interactions, *Nature Communications*, 14, 4045,  
880 <https://doi.org/10.1038/s41467-023-39794-7>, 2023.
- Lohmann, U. and Diehl, K.: Sensitivity Studies of the Importance of Dust Ice Nuclei for the Indirect Aerosol Effect on Stratiform Mixed-Phase Clouds, *Journal of the Atmospheric Sciences*, 63, 968–982, <https://doi.org/10.1175/jas3662.1>, 2006.
- MacMartin, D. G., Kravitz, B., Mills, M. J., Tribbia, J. J., Tilmes, S., Richter, J. H., Vitt, F., and Lamarque, J.-F.: The Climate Response to Stratospheric Aerosol Geoengineering Can Be Tailored Using Multiple Injection Locations, *Journal of Geophysical Research: Atmospheres*, 122, 12,574–12,590, <https://doi.org/10.1002/2017jd026868>, 2017.
- MacMartin, D. G., Vioni, D., Kravitz, B., Richter, J., Felgenhauer, T., Lee, W. R., Morrow, D. R., Parson, E. A., and Sugiyama, M.: Scenarios for modeling solar radiation modification, *Proceedings of the National Academy of Sciences*, 119, e2202230119, <https://doi.org/10.1073/pnas.2202230119>, 2022.



- Martínez Montero, M., Crucifix, M., Couplet, V., Brede, N., and Botta, N.: SURFER v2.0: a flexible and simple model linking anthropogenic  
890 CO<sub>2</sub> emissions and solar radiation modification to ocean acidification and sea level rise, *Geoscientific Model Development*, 15, 8059–  
8084, <https://doi.org/10.5194/gmd-15-8059-2022>, 2022.
- Mason, A. M., Henry, M., Hirasawa, H., O'Connor, F. M., and Haywood, J.: Assessing combinations of regional MCB designed to target  
multiple climate response objectives, *EGUsphere*, 2025, 1–29, 2025.
- McPartland, M. Y., Lovato, T., Koven, C. D., Wilson, J. D., Turner, B., Petrik, C. M., Licón-Saláiz, J., Li, F., Lhardy, F., Clement Kinney, J.,  
895 Kawamiya, M., Hassler, B., Gillett, N. P., Fall, C. M. N., Danek, C., Brierley, C. M., Bastos, A., and Andrews, O.: CMIP7 Data Request:  
Earth System Priorities and Opportunities, *EGUsphere*, 2025, 1–61, <https://doi.org/10.5194/egusphere-2025-3246>, 2025.
- Meinshausen, M., Schleussner, C.-F., Beyer, K., Bodeker, G., Boucher, O., Canadell, J. G., Daniel, J. S., Diongue-Niang, A., Driouech, F.,  
Fischer, E., Forster, P., Grose, M., Hansen, G., Hausfather, Z., Ilyina, T., Kikstra, J. S., Kimutai, J., King, A. D., Lee, J.-Y., Lennard, C.,  
Lissner, T., Nauels, A., Peters, G. P., Pirani, A., Plattner, G.-K., Pörtner, H., Rogelj, J., Rojas, M., Roy, J., Samset, B. H., Sanderson,  
900 B. M., Séférian, R., Seneviratne, S., Smith, C. J., Szopa, S., Thomas, A., Urge-Vorsatz, D., Velders, G. J. M., Yokohata, T., Ziehn, T., and  
Nicholls, Z.: A perspective on the next generation of Earth system model scenarios: towards representative emission pathways (REPs),  
*Geoscientific Model Development*, 17, 4533–4559, <https://doi.org/10.5194/gmd-17-4533-2024>, 2024.
- Moore, J. C., Mettiäinen, I., Wolovick, M., Zhao, L., Gladstone, R., Chen, Y., Kirchner, S., and Koivurova, T.: Targeted Geoengineering:  
Local Interventions with Global Implications, *Global Policy*, 12, 108–118, <https://doi.org/https://doi.org/10.1111/1758-5899.12867>, 2021.
- 905 Muñoz-Sánchez, R., Bastien-Olvera, B. A., Calderón, O., Estrada Porrúa, F., and Altamirano, M.: GeoMIP-Pattern –a pattern scaling dataset  
for efficient generation of custom geoengineering scenarios, *Scientific Data*, 12, 1343, 2025.
- Niemand, M., Möhler, O., Vogel, B., Vogel, H., Hoose, C., Connolly, P., Klein, H., Bingemer, H., DeMott, P., Skrotzki, J., and Leisner, T.: A  
Particle-Surface-Area-Based Parameterization of Immersion Freezing on Desert Dust Particles, *Journal of the Atmospheric Sciences*, 69,  
3077–3092, <https://doi.org/10.1175/jas-d-11-0249.1>, 2012.
- 910 Odoulami, R. C., Hirasawa, H., Kouadio, K., Patel, T. D., Quagraine, K. A., Pinto, I., Egbebiyi, T. S., Abiodun, B. J., Lennard, C., and New,  
M. G.: Africa's climate response to Marine Cloud Brightening strategies is highly sensitive to deployment region, *Journal of Geophysical  
Research: Atmospheres*, 129, e2024JD041 070, 2024.
- Palazzo Corner, S., Siebert, M., Ceppi, P., Fox-Kemper, B., Frñlicher, T. L., Gallego-Sala, A., Haigh, J., Hegerl, G. C., Jones, C. D., Knutti,  
R., Koven, C. D., MacDougall, A. H., Meinshausen, M., Nicholls, Z., SallÄ©e, J. B., Sanderson, B. M., SÄ©Ä©rian, R., Turetsky, M.,  
915 Williams, R. G., Zaehle, S., and Rogelj, J.: The Zero Emissions Commitment and climate stabilization, *Frontiers in Science*, Volume 1 -  
2023, <https://doi.org/10.3389/fsci.2023.1170744>, 2023.
- Parker, A. and Irvine, P. J.: The Risk of Termination Shock From Solar Geoengineering, *Earth's Future*, 6, 456–467,  
<https://doi.org/https://doi.org/10.1002/2017EF000735>, 2018.
- Pflüger, D., Wieners, C. E., van Kampenhout, L., Wijngaard, R. R., and Dijkstra, H. A.: Flawed Emergency Interven-  
920 tion: Slow Ocean Response to Abrupt Stratospheric Aerosol Injection, *Geophysical Research Letters*, 51, e2023GL106 132,  
<https://doi.org/https://doi.org/10.1029/2023GL106132>, e2023GL106132 2023GL106132, 2024.
- Pissoft, P., Sacha, P., Polvani, L. M., AÄ±el, J. A., de la Torre, L., Eichinger, R., Foelsche, U., Huszar, P., Jacobi, C., Karlicky, J., Kuchar,  
A., Miksovsky, J., Zak, M., and Rieder, H. E.: Stratospheric contraction caused by increasing greenhouse gases, *Environmental Research  
Letters*, 16, 064 038, <https://doi.org/10.1088/1748-9326/abfe2b>, 2021.
- 925 Plazzotta, M., Séférian, R., Douville, H., Kravitz, B., and Tjiputra, J.: Land Surface Cooling Induced by Sulfate Geoengineering Constrained  
by Major Volcanic Eruptions, *Geophysical Research Letters*, 45, 5663–5671, <https://doi.org/https://doi.org/10.1029/2018GL077583>, 2018.



- 930 Quaglia, I., Timmreck, C., Niemeier, U., Visioni, D., Pitari, G., Brodowsky, C., Brühl, C., Dhomse, S. S., Franke, H., Laakso, A., Mann, G. W., Rozanov, E., and Sukhodolov, T.: Interactive stratospheric aerosol models' response to different amounts and altitudes of SO<sub>2</sub> injection during the 1991 Pinatubo eruption, *Atmospheric Chemistry and Physics*, 23, 921–948, <https://doi.org/10.5194/acp-23-921-2023>, 2023.
- Rasch, P. J., Latham, J., and Chen, C.-C. J.: Geoengineering by cloud seeding: influence on sea ice and climate system, *Environmental Research Letters*, 4, 045 112, 2009.
- Rasch, P. J., Hirasawa, H., Wu, M., Doherty, S. J., Wood, R., Wang, H., Jones, A., Haywood, J., and Singh, H.: A protocol for model intercomparison of impacts of marine cloud brightening climate intervention, *Geoscientific Model Development*, 17, 7963–7994, 2024.
- 935 Richter, J.: ARISE-SAI-1.5, <https://gdex.ucar.edu/datasets/d651059/>, 2025.
- Richter, J., Visioni, D., MacMartin, D., Bailey, D., Rosenbloom, N., Lee, W., Tye, M., and Lamarque, J.-F.: Assessing Responses and Impacts of Solar climate intervention on the Earth system with stratospheric aerosol injection (ARISE-SAI), *EGUsphere*, 2022, 1–35, <https://doi.org/10.5194/egusphere-2022-125>, 2022.
- Robock, A., Oman, L., and Stenchikov, G. L.: Regional climate responses to geoengineering with tropical and Arctic SO<sub>2</sub> injections, *Journal of Geophysical Research: Atmospheres*, 113, <https://doi.org/https://doi.org/10.1029/2008JD010050>, 2008.
- 940 Sanderson, B. M., Brovkin, V., Fisher, R. A., Hohn, D., Ilyina, T., Jones, C. D., Koenigk, T., Koven, C., Li, H., Lawrence, D. M., Lawrence, P., Liddicoat, S., MacDougall, A. H., Mengis, N., Nicholls, Z., O'Rourke, E., Romanou, A., Sandstad, M., Schwinger, J., Séférian, R., Sentman, L. T., Simpson, I. R., Smith, C., Steinert, N. J., Swann, A. L. S., Tjiputra, J., and Ziehn, T.: flat10MIP: an emissions-driven experiment to diagnose the climate response to positive, zero and negative CO<sub>2</sub> emissions, *Geoscientific Model Development*, 18, 5699–5724, <https://doi.org/10.5194/gmd-18-5699-2025>, 2025.
- Schwalm, C. R., Glendon, S., and Duffy, P. B.: RCP8.5 tracks cumulative CO<sub>2</sub> emissions, *Proceedings of the National Academy of Sciences*, 117, 19 656–19 657, <https://doi.org/10.1073/pnas.2007117117>, 2020.
- Simpson, I., Tilmes, S., Richter, J., Kravitz, B., MacMartin, D., Mills, M., Fasullo, J., and Pendergrass, A.: The regional hydroclimate response to stratospheric sulfate geoengineering and the role of stratospheric heating, *Journal of Geophysical Research: Atmospheres*, 950 124, 2019JD031 093, <https://doi.org/10.1029/2019JD031093>, 2019.
- Smith, W.: An assessment of the infrastructural and temporal barriers constraining a near-term implementation of a global stratospheric aerosol injection program, *Environmental Research Communications*, 6, 061 007, <https://doi.org/10.1088/2515-7620/ad4f5c>, 2024.
- Smith, W., Bartels, M. F., Boers, J. G., and Rice, C. V.: On Thin Ice: Solar Geoengineering to Manage Tipping Element Risks in the Cryosphere by 2040, *Earth's Future*, 12, e2024EF004 797, <https://doi.org/10.1029/2024EF004797>, \_eprint: <https://onlinelibrary.wiley.com/doi/pdf/10.1029/2024EF004797>, 2024.
- 955 Stefanetti, F., Vattioni, S., Dykema, J. A., Chiodo, G., Sedlacek, J., Keutsch, F. N., and Sukhodolov, T.: Stratospheric injection of solid particles reduces side effects on circulation and climate compared to SO<sub>2</sub> injections, *Environmental Research: Climate*, 3, <https://doi.org/10.1088/2752-5295/ad9f93>, 2024.
- Stengel, M., Stapelberg, S., Sus, O., Finkensieper, S., Würzler, B., Philipp, D., Hollmann, R., Poulsen, C., Christensen, M., and McGarragh, 960 G.: Cloud\_cci Advanced Very High Resolution Radiometer post meridiem (AVHRR-PM) dataset version 3: 35-year climatology of global cloud and radiation properties, *Earth System Science Data*, 12, 41–60, <https://doi.org/10.5194/essd-12-41-2020>, 2020.
- Stjern, C. W., Muri, H., Ahlm, L., Boucher, O., Cole, J. N., Ji, D., Jones, A., Haywood, J., Kravitz, B., Lenton, A., et al.: Response to marine cloud brightening in a multi-model ensemble, *Atmospheric Chemistry and Physics*, 18, 621–634, 2018.



- Sun, H., Bourguet, S., Eastham, S., and Keith, D.: Optimizing Injection Locations Relaxes Altitude-Lifetime Trade-Off for Strato-  
965 spheric Aerosol Injection, *Geophysical Research Letters*, 50, e2023GL105371, <https://doi.org/10.1029/2023GL105371>, <https://onlinelibrary.wiley.com/doi/pdf/10.1029/2023GL105371>, 2023.
- Sun, L., Hurrell, J. W., Rasmussen, K. L., Summers, B., Sherman, E. A., and Kravitz, B.: Assessing the Impact of Solar Climate Intervention  
on Future US Weather Using a Convection-Permitting WRF Model, *EGUsphere*, 2025, 1–29, 2025.
- Sun, L., Hurrell, J. W., Rasmussen, K. L., Summers, B., Sherman, E. A., and Kravitz, B.: Assessing the impact of solar climate in-  
970 tervention on future U.S. weather using a convection-permitting WRF model, *Geoscientific Model Development*, 19, 2239–2256,  
<https://doi.org/10.5194/gmd-19-2239-2026>, 2026.
- Tilmes, S., MacMartin, D. G., Lenaerts, J. T. M., van Kampenhout, L., Muntjewerf, L., Xia, L., Harrison, C. S., Krumhardt, K. M., Mills,  
M. J., Kravitz, B., and Robock, A.: Reaching 1.5 and 2.0C global surface temperature targets using stratospheric aerosol geoengineering,  
*Earth System Dynamics*, 11, 579–601, <https://doi.org/10.5194/esd-11-579-2020>, 2020.
- 975 Tilmes, S., Visionsi, D., Jones, A., Haywood, J., Séférian, R., Nabat, P., Boucher, O., Bednarz, E. M., and Niemeier, U.: Stratospheric ozone  
response to sulfate aerosol and solar dimming climate interventions based on the G6 Geoengineering Model Intercomparison Project  
(GeoMIP) simulations, *Atmospheric Chemistry and Physics*, 22, 4557–4579, <https://doi.org/10.5194/acp-22-4557-2022>, 2022.
- Tilmes, S., Rosenlof, K. H., Visionsi, D., Bednarz, E. M., Felgenhauer, T., Smith, W., Lennard, C., Diamond, M. S., Henry, M., Harrison, C. S.,  
and Thompson, C.: Research criteria towards an interdisciplinary Stratospheric Aerosol Intervention assessment, *Oxford Open Climate*  
980 *Change*, 4, kgae010, <https://doi.org/10.1093/oxfclm/kgae010>, 2024.
- Tilmes, S., Bednarz, E. M., Jörmann, A., Visionsi, D., Kinnison, D. E., Chiodo, G., and Plummer, D.: Stratospheric Aerosol Intervention  
experiment for the Chemistry–Climate Model Initiative, *Atmospheric Chemistry and Physics*, 25, 6001–6023, <https://doi.org/10.5194/acp-25-6001-2025>, 2025.
- Tilmes, S., Visionsi, D., Quaglia, I., Zhu, Y., Bardeen, C. G., Vitt, F., and Yu, P.: Uncertainties of SAI efficiency and impacts depending on  
985 the complexity of the aerosol microphysical model, *Atmospheric Chemistry and Physics*, 26, 2649–2666, <https://doi.org/10.5194/acp-26-2649-2026>, 2026.
- Toll, V., Rahu, J., Keernik, H., Trofimov, H., Voormansik, T., Manshausen, P., Hung, E., Michelson, D., Christensen, M. W., Post,  
P., Junninen, H., Murray, B. J., Lohmann, U., Watson-Parris, D., Stier, P., Donaldson, N., Storelvmo, T., Kulmala, M., and Bel-  
louin, N.: Glaciation of liquid clouds, snowfall, and reduced cloud cover at industrial aerosol hot spots, *Science*, 386, 756–762,  
990 <https://doi.org/10.1126/science.adl0303>, 2024.
- Trisos, C. H., Amatulli, G., Gurevitch, J., Robock, A., Xia, L., and Zambri, B.: Potentially dangerous consequences for biodiversity of solar  
geoengineering implementation and termination, *Nature Ecology & Evolution*, 2, 475–482, <https://doi.org/10.1038/s41559-017-0431-0>,  
2018.
- Tye, M. R., Dagon, K., Molina, M. J., Richter, J. H., Visionsi, D., Kravitz, B., and Tilmes, S.: Indices of extremes: geographic pat-  
995 terns of change in extremes and associated vegetation impacts under climate intervention, *Earth System Dynamics*, 13, 1233–1257,  
<https://doi.org/10.5194/esd-13-1233-2022>, 2022.
- van Vuuren, D., O’Neill, B., Tebaldi, C., Chini, L., Friedlingstein, P., Hasegawa, T., Riahi, K., Sanderson, B., Govindasamy, B., Bauer, N.,  
Eyring, V., Fall, C., Frieler, K., Gidden, M., Gohar, L., Jones, A., King, A., Knutti, R., Kriegler, E., Lawrence, P., Lennard, C., Lowe, J.,  
Mathison, C., Mehmood, S., Prado, L., Zhang, Q., Rose, S., Ruane, A., Schleussner, C.-F., Seferian, R., Sillmann, J., Smith, C., Sörensson,  
1000 A., Panickal, S., Tachiiri, K., Vaughan, N., Vishwanathan, S., Yokohata, T., and Ziehn, T.: The Scenario Model Intercomparison Project  
for CMIP7 (ScenarioMIP-CMIP7), *EGUsphere*, 2025, 1–38, <https://doi.org/10.5194/egusphere-2024-3765>, 2025.



- Vattioni, S., Luo, B., Feinberg, A., Stenke, A., Vockenhuber, C., Weber, R., Dykema, J. A., Krieger, U. K., Ammann, M., Keutsch, F., Peter, T., and Chiodo, G.: Chemical Impact of Stratospheric Alumina Particle Injection for Solar Radiation Modification and Related Uncertainties, *Geophysical Research Letters*, 50, e2023GL105 889, <https://doi.org/10.1029/2023GL105889>, 2023.
- 1005 Vattioni, S., Käslin, S. K., Dykema, J. A., Beiping, L., Sukhodolov, T., Sedlacek, J., Keutsch, F. N., Peter, T., and Chiodo, G.: Microphysical Interactions Determine the Effectiveness of Solar Radiation Modification via Stratospheric Solid Particle Injection, *Geophysical Research Letters*, 51, e2024GL110 575, <https://doi.org/https://doi.org/10.1029/2024GL110575>, 2024a.
- Vattioni, S., Weber, R., Feinberg, A., Stenke, A., Dykema, J. A., Luo, B., Kelesidis, G. A., Bruun, C. A., Sukhodolov, T., Keutsch, F. N., Peter, T., and Chiodo, G.: A fully coupled solid-particle microphysics scheme for stratospheric aerosol injections within the aerosol–chemistry–climate model SOCOL-AERv2, *Geoscientific Model Development*, 17, 7767–7793, <https://doi.org/10.5194/gmd-17-7767-2024>, 2024b.
- 1010 Vattioni, S., Peter, T., Weber, R., Dykema, J. A., Luo, B., Stenke, A., Feinberg, A., Sukhodolov, T., Keutsch, F. N., Ammann, M., Vockenhuber, C., Döbeli, M., Kelesidis, G. A., and Chiodo, G.: Injecting solid particles into the stratosphere could mitigate global warming but currently entails great uncertainties, *Communications Earth and Environment*, 6, <https://doi.org/10.1038/s43247-025-02038-1>, 2025.
- 1015 Villanueva, D., Possner, A., Neubauer, D., Gasparini, B., Lohmann, U., and Tesche, M.: Mixed-phase regime cloud thinning could help restore sea ice, *Environmental Research Letters*, 17, 114 057, <https://doi.org/10.1088/1748-9326/aca16d>, 2022.
- Villanueva, D., Stengel, M., Hoose, C., Bruno, O., Jeggle, K., Ansmann, A., and Lohmann, U.: Dust-driven droplet freezing explains cloud-top phase in the northern extratropics, *Science*, 389, 521–525, <https://doi.org/10.1126/science.adt5354>, 2025.
- Villanueva, D., Farron, P., Vella, R., and Hirasawa, H.: Level 0 data from the model intercomparison of Mixed-Phase Cloud Thinning included in "The Geoengineering Model Intercomparison Project (GeoMIP) contribution to CMIP7", <https://doi.org/10.5281/zenodo.19665403>, 2026.
- 1020 Visionsi, D., MacMartin, D. G., and Kravitz, B.: Is Turning Down the Sun a Good Proxy for Stratospheric Sulfate Geoengineering?, *Journal of Geophysical Research: Atmospheres*, 126, e2020JD033 952, <https://doi.org/https://doi.org/10.1029/2020JD033952>, e2020JD033952 2020JD033952, 2021a.
- 1025 Visionsi, D., MacMartin, D. G., Kravitz, B., Boucher, O., Jones, A., Lurton, T., Martine, M., Mills, M. J., Nabat, P., Niemeier, U., Séférian, R., and Tilmes, S.: Identifying the sources of uncertainty in climate model simulations of solar radiation modification with the G6sulfur and G6solar Geoengineering Model Intercomparison Project (GeoMIP) simulations, *Atmospheric Chemistry and Physics*, 21, 10 039–10 063, <https://doi.org/10.5194/acp-21-10039-2021>, 2021b.
- Visionsi, D., Bednarz, E. M., Lee, W. R., Kravitz, B., Jones, A., Haywood, J. M., and MacMartin, D. G.: Climate response to off-equatorial stratospheric sulfur injections in three Earth system models – Part 1: Experimental protocols and surface changes, *Atmospheric Chemistry and Physics*, 23, 663–685, <https://doi.org/10.5194/acp-23-663-2023>, 2023a.
- 1030 Visionsi, D., Bednarz, E. M., MacMartin, D. G., Kravitz, B., and Goddard, P. B.: The Choice of Baseline Period Influences the Assessments of the Outcomes of Stratospheric Aerosol Injection, *Earth's Future*, 11, e2023EF003 851, <https://doi.org/https://doi.org/10.1029/2023EF003851>, e2023EF003851 2023EF003851, 2023b.
- 1035 Visionsi, D., Kravitz, B., Robock, A., Tilmes, S., Haywood, J., Boucher, O., Lawrence, M., Irvine, P., Niemeier, U., Xia, L., Chiodo, G., Lennard, C., Watanabe, S., Moore, J. C., and Muri, H.: Opinion: The scientific and community-building roles of the Geoengineering Model Intercomparison Project (GeoMIP) – past, present, and future, *Atmospheric Chemistry and Physics*, 23, 5149–5176, <https://doi.org/10.5194/acp-23-5149-2023>, 2023c.



- 1040 Visioni, D., Robock, A., Haywood, J., Henry, M., Tilmes, S., MacMartin, D. G., Kravitz, B., Doherty, S. J., Moore, J., Lennard, C., Watanabe, S., Muri, H., Niemeier, U., Boucher, O., Syed, A., Egbebiyi, T. S., Séférian, R., and Quaglia, I.: G6-1.5K-SAI: a new Geoengineering Model Intercomparison Project (GeoMIP) experiment integrating recent advances in solar radiation modification studies, *Geoscientific Model Development*, 17, 2583–2596, <https://doi.org/10.5194/gmd-17-2583-2024>, 2024.
- 1045 Visioni, D., Robock, A., Roberts, K. E., Lee, W., Henry, M., Duffey, A., Hirasawa, H., Chegwidan, O., and Sipra, H.: Finalizing Experimental Protocols for the Geoengineering Model Intercomparison Project (GeoMIP) Contribution to CMIP7, *Bulletin of the American Meteorological Society*, 106, E2029 – E2035, <https://doi.org/10.1175/BAMS-D-25-0191.1>, 2025.
- Wang, C., Visioni, D., Chua, G., and Bednarz, E. M.: Air quality impacts of stratospheric aerosol injections are likely small and mainly driven by changes in climate, not aerosol settling, *Atmospheric Chemistry and Physics*, 26, 1339–1357, <https://doi.org/10.5194/acp-26-1339-2026>, 2026.
- 1050 Wang, J., Moore, J. C., Zhao, L., Yue, C., and Di, Z.: Regional dynamical and statistical downscaling temperature, humidity and wind-speed for the Beijing region under stratospheric aerosol injection geoengineering, *Earth System Dynamics Discussions*, 2022, 1–33, <https://doi.org/10.5194/esd-2022-35>, 2022.
- Weisenstein, D. K., Visioni, D., Franke, H., Niemeier, U., Vattioni, S., Chiodo, G., Peter, T., and Keith, D. W.: A Model Intercomparison of Stratospheric Solar Geoengineering by Accumulation-Mode Sulfate Aerosols, *Atmospheric Chemistry and Physics Discussions*, 2021, 1–30, 2021.
- 1055 Wells, A. F. and Haywood, J. M.: A Risk-Risk Assessment of Climate Extremes: Comparing Greenhouse Gas Warming and Stratospheric Aerosol Injection in UKESM1, *Earth's Future*, 13, e2024EF005810, <https://doi.org/https://doi.org/10.1029/2024EF005810>, e2024EF005810 2024EF005810, 2025.
- 1060 Wheeler, L., Wagman, B., Smith, W., Davies, P., Cook, B., Brunell, S., Glen, A., Hackenburg, D., Lien, J., Shand, L., and Zeitler, T.: Design and simulation of a logistically constrained high-latitude, low-altitude stratospheric aerosol injection scenario in the Energy Exascale Earth System Model (E3SM), *Environmental Research Letters*, 20, 044011, <https://doi.org/10.1088/1748-9326/adba01>, publisher: IOP Publishing, 2025.
- 1065 Winkelmann, R., Dennis, D. P., Donges, J. F., Loriani, S., Klose, A. K., Abrams, J. F., Alvarez-Solas, J., Albrecht, T., Armstrong McKay, D., Bathiany, S., Blasco Navarro, J., Brovkin, V., Burke, E., Danabasoglu, G., Donner, R. V., Drüke, M., Georgievski, G., Goelzer, H., Harper, A. B., Hegerl, G., Hirota, M., Hu, A., Jackson, L. C., Jones, C., Kim, H., Koenigk, T., Lawrence, P., Lenton, T. M., Liddy, H., Licón-Saláiz, J., Menthon, M., Montoya, M., Nitzbon, J., Nowicki, S., Otto-Bliesner, B., Pausata, F., Rahmstorf, S., Ramin, K., Robinson, A., Rockström, J., Romanou, A., Sakschewski, B., Schädel, C., Sherwood, S., Smith, R. S., Steinert, N. J., Swingedouw, D., Willeit, M., Weijer, W., Wood, R., Wyser, K., and Yang, S.: The Tipping Points Modelling Intercomparison Project (TIPMIP): Assessing tipping point risks in the Earth system, *EGUsphere*, 2025, 1–52, <https://doi.org/10.5194/egusphere-2025-1899>, 2025.
- 1070 Wood, R.: Assessing the potential efficacy of marine cloud brightening for cooling Earth using a simple heuristic model, *Atmospheric Chemistry and Physics Discussions*, 2021, 1–52, 2021.
- Wunderlin, E., Chiodo, G., Sukhodolov, T., Vattioni, S., Visioni, D., and Tilmes, S.: Side Effects of Sulfur-Based Geoengineering Due To Absorptivity of Sulfate Aerosols, *Geophysical Research Letters*, 51, <https://doi.org/10.1029/2023GL107285>, 2024.
- 1075 Zanchettin, D., Timmreck, C., Khodri, M., Schmidt, A., Toohey, M., Abe, M., Bekki, S., Cole, J., Fang, S.-W., Feng, W., Hegerl, G., Johnson, B., Lebas, N., LeGrande, A. N., Mann, G. W., Marshall, L., Rieger, L., Robock, A., Rubinetti, S., Tsigaridis, K., and Weierbach, H.: Effects of forcing differences and initial conditions on inter-model agreement in the VolMIP volc-pinatubo-full experiment, *Geoscientific Model Development*, 15, 2265–2292, <https://doi.org/10.5194/gmd-15-2265-2022>, 2022.



- Zarnetske, P. L., Gurevitch, J., Franklin, J., Groffman, P. M., Harrison, C. S., Hellmann, J. J., Hoffman, F. M., Kothari, S., Robock, A., Tilmes, S., Vioni, D., Wu, J., Xia, L., and Yang, C.-E.: Potential ecological impacts of climate intervention by reflecting sunlight to cool Earth, *Proceedings of the National Academy of Sciences*, 118, <https://doi.org/10.1073/pnas.1921854118>, 2021.
- 1080 Zhang, Y., MacMartin, D. G., Vioni, D., and Kravitz, B.: How large is the design space for stratospheric aerosol geoengineering?, *Earth System Dynamics*, 13, 201–217, <https://doi.org/10.5194/esd-13-201-2022>, publisher: Copernicus GmbH, 2022.
- Zhao, M., Cao, L., Vioni, D., and MacMartin, D. G.: Carbon Cycle Response to Stratospheric Aerosol Injection With Multiple Temperature Stabilization Targets and Strategies, *Earth's Future*, 12, e2024EF004 474, <https://doi.org/https://doi.org/10.1029/2024EF004474>, e2024EF004474 2024EF004474, 2024.
- 1085 Zhao, M., Cao, L., Vioni, D., and MacMartin, D. G.: Response of Tipping Elements to Different Strategies of Stratospheric Aerosol Injection, *Earth's Future*, 13, e2025EF006 736, <https://doi.org/https://doi.org/10.1029/2025EF006736>, e2025EF006736 2025EF006736, 2025.